Bae Institute
Advanced Space and Medical Technologies

NIAC
NASA Institute for Advanced Concepts

A Contamination-Free Ultrahigh Precision Formation Flight Method Based on Intracavity Photon Thrusters and Tethers: Photon Tether Formation Flight (PTFF)

Phase I Program 07605-003-041

Phase I Final Report

Prepared for:
Robert A. Cassanova, Ph.D., Director
NASA Institute for Advanced Concepts

April 30, 2006

PI: Young K. Bae, Ph.D.
BAE INSTITUTE

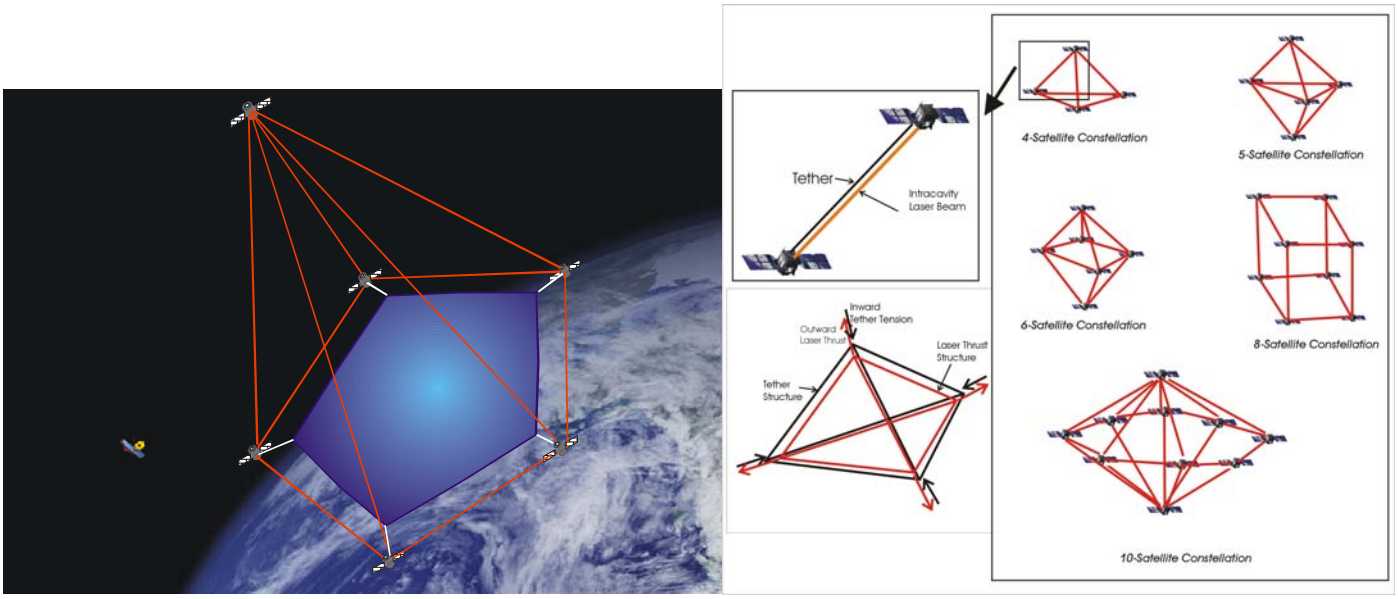

"I believe in intuitions and inspirations.
I sometimes feel that I am right.
I do not know that I am."

by Albert Einstein

CONTRIBUTORS

Young K. Bae, Ph.D.	Bae Institute
C. William Larson, Ph.D,	Air Force Research Laboratory
T. Precilla, Ph.D.	Northrop Grumman
Joseph Carroll	Tether Applications Inc.
Claude Phipps, Ph.D.	Photonics Associates

Cover: An artist's concept of a km-diameter ultralarge membrane telescope formed by spacecraft in nano-precision formation flying (not to scale). A small space telescope shown left side is an artist's concept of James Webb Space Telescope for size comparison. The second panel shows the general force structure of formation flying and examples of nano-precision structures that can be formed with the proposed method.

TABLE OF CONTENTS

OVERVIEW

We proposed a revolutionary nano-meter accuracy formation flight method based on photon thrusters and tethers, **Photon Tether Formation Flight (PTFF)**, with the maximum baseline distance over 10 km, and have investigated its feasibility in depth during this project. In addition, PTFF is predicted to be able to provide an angular scanning accuracy of 0.1 micro-arcsec, and the retargeting slewing accuracy better than 1 micro-arcsec for a 1 km baseline formation.

The conclusion of this study is that the implementation of the proposed method in the near future is well within reach of the present technologies. Therefore, we are confident that the proposed PTFF needs thorough continued study that will establish a reliable technical path to the launch of an exciting new class of NASA space mission. In this report, we review how we arrived at the conclusion and the scientific and technological potential of the method, and show how it can be realized and implemented in numerous NASA space missions. We present some instrument design concepts for PTFF and analysis of their technological readiness in terms of the NASA TRL scale. From these we identify which are the key technologies that need attention before the proposed method is implemented in a mission with confidence.

The core technology of PTFF is in the strategic combination of photon thrusters and tethers, which provides propellant-free, thus contamination-free, ultrahigh precision control. The intracavity arrangement was exploited to trap photons between two spacecraft multiplying the thrust by several orders of magnitudes. As a result, the thrust power requirement for formation of 100 kg spacecrafts can be only several watts per pair, within the power budget. The intracavity arrangement further allows ultrahigh precision thrust vector control that cannot be achieved with the conventional thrusters. Propellant mass saving and longer mission lifetime (tens of years) are other advantages of the proposed concept.

Furthermore, a portion of ultra-stable photon thruster lasers can be used for nano-meter accuracy interferometric ranging simplifying the system design and reducing the system weight. This approach also eliminates the necessity of additional optical delay line system that was necessary in the existing formation flying methods, thus it results in further weight reduction and system simplification. In addition, PTFF is capable of providing near adiabatic CW control that minimizes generation of tether vibration. Tether vibrations potentially caused by meteoroid impact and major formation structure reorientation, have been addressed and shown to be readily quenched with electromechanical dampers and photon thruster power modulation.

In addition to redefining and simplifying the existing NASA mission concepts, such as SPECS and MAXIM, PTFF enables other emerging revolutionary mission concepts, such as New World Imager Freeway Mission proposed by Prof. Cash, which searches for advanced civilization and in exo-planets Fourier Transform X-Ray Spectrometer proposed by Dr. Schnopper. As the present concept is more publicized, many other exciting concepts are expected to be inspired by PTFF. One of such possible NASA missions is the construction of ultralarge space telescope with diameters up to several km for observing and monitoring space and earth-bound activities.

I. INTRODUCTION

In recent years, microsatellites and nanosatellites enables the insertion of sophisticated sensors and processing technologies into orbits of interest at low costs (Leitner, 2004) for the next generation NASA missions. Building a cluster of small satellites has been recognized to be more affordable, robust and versatile than building a large monolithic satellite. Specifically, the grouped satellite cluster is crucial for enabling orders-of-magnitude improvements in resolution and coverage achievable from advanced remote sensing platforms. Size limitations on launch vehicle fairings leave formation flying as the only option to assimilate coherent large apertures or large sample collection areas in space (Leitner, 2004).

Numerous NASA mission applications have been envisioned; for example, the ultrahigh precision satellite clusters can eable interferometry and distributed large aperture sensors, especially at optical (TPF, and SPECS) and x-ray wavelengths (MAXIM) (Leisawitz, 2004, Cash, 2002). For non-NASA applications, the proposed system can enable advanced geophysical monitoring where GPS and standard laser range finders are currently inadequate to measure and monitor small changes in the movement of earthquake plates, and gravity wave detection. Other commercial and military applications include distributed large aperture optical and infrared sensors for ultrahigh resolution monitoring and imaging at low-cost.

Such a technology critically depends on the formation flying method that enables precision spacecraft formation keeping from coarse requirements (relative position control of any two spacecraft to less than 1 cm, and relative bearing of 1 arcmin over target range of separations from a few meters to tens of kilometers) to fine requirements (nanometer relative position control). For example, one of the most challenging applications for formation flying thus so far is that of the proposed x-ray interferometry for space imaging applications, MAXIM (Cash, 2000). The concept has evolved to include a pathfinder mission, consisting of a single x-ray interferometer and a trailing imaging satellite, and the full MAXIM, consisting of a fleet of 33 x-ray mirror satellites, a trailing collector satellite, and an imaging or detector spacecraft.

The formation flying baseline accuracy for optical interferometry applications can be relaxed with the use of optical delay lines (ODL) as has been proposed in the existing formation flying concepts. However, this concept requires two independent systems, the spacecraft position control system and optical delay line control system, for controlling two different types of random motions of which magnitudes are several orders of magnitude different. Therefore, the control system would be exceedingly technologically challenging. Another simpler approach to this problem is the use of the spacecraft platform as optical platforms. Although this approach highly simplifies the system integration and reduces the weight, it requires the baseline control accuracy that

are much more stringent than that can be obtained with the conventional control method with traditional thrusters. In this case, summary of the requirement of the baseline accuracy tolerance of several exemplary missions compared with the capability of the present formation flying method is shown in Fig. 1.

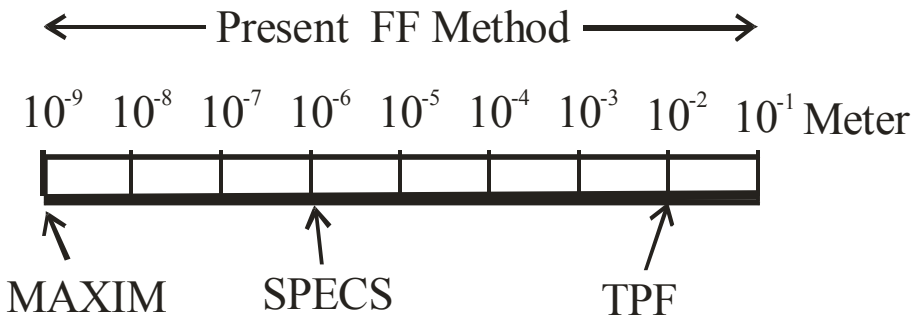

FIGURE 1. Required Base Line Accuracy of Several Exemplary NASA Missions and the Capability of the Present FF Method. The accuracy is estimated for the system without the optical delay line system.

In MAXIM, the relative distance between the hub satellite and collector satellites should be precisely maintained with the tolerance of a few nm (10^{-9} m) at the distance of 200 m, and the precision requirement in maintaining the distance, thus, is 10 parts per trillion, one of the most stringent accuracy requirement seen in any scientific fields. In addition, potential contamination of neighboring spacecraft by propellant exhaust plumes and the possibility of pulsed electromagnetic interference with low power inter-satellite communications remain a real concern for grouped satellite clusters. These requirements essentially rule out the usage of the most of the conventional propellant based propulsion systems, such as gas hydrazine thrusters, pulsed plasma thrusters, hall thrusters, electrostatic ion engines, and field emission electron propulsion systems.

To alleviate the second critical concern, the propellant plume contamination, several propellant-free formation flying methods have been proposed. The propulsive conducting tethers and spin-stabilized tether systems have been proposed in place of on-board propulsion systems to form and maintain satellite formations (Johnson, 1998, Quinn, 2000). While such concepts offer intriguing possibilities for small arrays consisting of only a few spacecraft, implementing a system for dozens of satellites quickly becomes extremely problematic. Several other new concepts have been proposed. They are: 1) the microwave scattering concept (LaPointe, 2001), 2) Coulomb force concept (King, 2002), 3) magnetic dipole interaction concept (Miller, 2003). In the microwave scattering formation flight method (LaPointe, 2001), radiation forces on the order of 10^{-9} N/W may be generated using electromagnetic gradient forces or scattering forces; microwave beam powers of 10-kW can thus produce restoring forces of approximately 10-μN, which are sufficient to correct a number of orbital perturbations. It requires very high power consumption, and focusing of the microwave requires larger

antenna arrays, and the scattered microwaves may electronically interfere with other neighboring satellites. The Coulomb control system (King, 2002) is limited to close formation flying in plasma environments characterized by Debye lengths greater than inter-vehicle separation. Even for such formations, however, the Coulomb control forces become negligible for separations greater than 50 m. It is apparent that more traditional thrusters would be necessary for formation keeping over larger distances. Generating usable Coulomb control forces requires charging spacecraft to high voltages, thus great care must be taken in vehicle design to prevent differential charging and instrument damage due to electrostatic discharge. In the magnetic dipole concept (Miller, 2003), two technical challenges should be overcome: 1) it may not work at the distances greater than tens of meters, thus cannot be used for SPECS and MAXIM, 2) the system can be extremely bulky and heavy (tons). Therefore, searches continue for the concept that does not require propellant nor extreme high voltages, and is power efficient and light.

Even if an efficient propellant-free thrust is developed, for ultrahigh precision formation flying, the issue of thrust pointing, the method of controlling thrust to the desired accuracy, the precision ranging metrology and the overall system architecture should be addressed. Thus far, a solution for maintaining a precise spacecraft configuration that can be used as an optical platform in space has proven illusive.

We have proposed and investigated under this NIAC Phase I contract the feasibility of a potentially revolutionary formation flying method, Photon Tether Formation Flight (**PTFF**), which enables ultrahigh precision spacecraft/satellite formation flying with intersatellite distance accuracy of nm (10^{-9} m) at maximum estimated distances in the order of tens of km in principle. The method is based on an innovative ultrahigh precision intracavity photon thruster able to provide continuously adjustable thrust from pN (10^{-12} N) to mN between spacecraft/satellites, and tethers. The thrust of the photons are amplified by as much as 20,000 times by bouncing them between two mirrors located separately between pairing satellites, and a 10 W photon thruster, which is suitable for microsatellite formation flying, is capable of providing thrusts up to 1.34 mN with currently available components. This thruster efficiency well rivals that of the most efficient electric propulsion system. A crystalline-like structure of satellites is proposed to be formed by the pushing-out force of the intracavity lasers and the pulling-in force of the tether tension between satellites.

The salient features of the present concept are:

- The proposed photon thruster system is capable of generating propellant-free continuously for tens of years,
- In combination of a tether system, the proposed photon thruster is capable of controlling and maintaining continuously the intersatellite distance with an accuracy better than nanometer,

- The dual usage of the photon thruster as a laser source for the ultrahigh precision interferometric ranging system simplifies the system architecture and control, and minimizes the system weight and power consumption,
- The thrust vector can be defined with ultrahigh precision due to the nature of the laser cavity.
- The method can be readily scaled down to nano- and pico-satellite formation flying.

Ever since the concept was proposed, though there seems to be no violation of physical principles in the concept, numerous daunting engineering challenges have emerged. It seems that more engineering problems will be identified as the program progresses. The challenging engineering problems identified so far can be classified into three categories:

1. The photon thruster system issues
   - The practical limit on operation distance of the proposed concept
   - The practical limit on the reflectance of the mirrors
   - Thermal management of the laser system, in particular, that of the laser crystal in the cavity
   - The method to provide maximum dynamic range with maximum distance precision
   - The operational lifetime of the laser system and how to extend it
   - The method of the pointing system to align the laser beam

1. The tether system issues
   - The hardware to control/adjust the length
   - The method to damp vibrations or resonances in the tethers
   - The method to adjust the thermal expansion/contraction
   - The lifetime of the tethers in the space environment
   - The method of coping the breakage of tethers due to micrometeoroid impact

2. Coordination of photon thrusters with tethers and overall system control issues
   - The method to compensate various perturbations, such as the solar pressure, drag force, thermal expansion/contraction, in the space environment
   - The method to obtain ultrahigh precision relative position information of satellites
   - The engineering architecture of the multiple satellite system
   - The control/command method

During this Phase I NIAC program, we have investigated these issues, and concluded that the proposed concept is indeed feasible. Many of these technical and engineering issues have been tackled during Phase I study, and we plan to continue this effort in Phase II. The following sections summarize the results of the study.

II. PHOTON TETHER FORMATION FLIGHT (PTFF)

A. General System Concept

The Photon Tether Formation Flight (**PTFF**) enables ultrahigh precision satellite formation flying with intersatellite distance accuracy of nm (10^{-9} m) at maximum estimated distances in the order of tens of km. Thus, the present method can be used for most of next generation NASA formation flying missions envisioned so far, including TPF, SPECS, and MAXIM without the complication of the optical delay lines. The method is based on innovative ultrahigh precision laser intracavity thrusters able to provide continuously adjustable precision CW thrust between microsatellites and tethers.

The present concept can be used for both spinning and non-spinning systems. In slowly spinning systems, as in NASA SPECS, centrifugal force can provide a precise repulsive force, allowing a low-mass tether to provide precise control of distance. There is a problem how quickly that force can be adjusted without risk of inducing undesired resonances, and to solve the problem, the agile control loop can use adjustable laser power rather than mechanical tether length control as the primary control mechanism. In non-spinning systems centrifugal force is not available, and a laser will provide the major repulsive force. In both spinning and non-spinning cases, the fast feedback possible can be used not just to control position, but to reduce the required agility of the tether control, and hence the problems induced by undesired tether resonances.

The schematic diagram of the proposed concept is shown in Fig. 2. Specifically, the proposed formation flying method is based on pulling-in force provided by tether tension and the pushing-apart CW thrust of the intracavity photon thruster. Although the thrust produced by single bounces of photons is typically negligibly small, the intracavity geometry allows photons to bounce between two mirrors as many times as tens of thousands, resulting in several orders of magnitude amplification of the thrust with a given laser power. With this proposed method, we estimate the distance between the satellite pairs in the constellation structure can be adjusted and maintained rapidly to the accuracy of nanometer. The photon thrust and tension of tethers form the backbone linear force structure of the crystalline-like structured formation flying, and can rapidly damp the perturbation from the space environmental sources, such as solar pressure, drag-force, and temperature fluctuation, applied from any direction.

Several exemplary structures and the general force structure are illustrated in Fig. 2. For example, the tetrahedral structural can be used for NASA SPECS applications. As illustrated in Fig. 2, the present concept “inflate” the ultralarge space structure with bouncing photons, and the structure boundary is limited and stabilized by tethers. For NASA MAXIM applications, an elongated polygon bipyramidal structure similar to the 10 satellites constellation can be used, except instead of 8 satellites 32 collector

spacecrafts will be used in the plane. The apex will be occupied by the hub and converger crafts. The approximate distance between the collector and hub crafts is about 100 m, and that between the collector and the converger crafts is about 10 km. This is slightly modified structure from the original one (Cash, 2000). These numbers will be used to estimate the necessary operation parameters in the later sections. For one to two dimensional structures, such as in ST-3 and space Fourier Transform X-Ray Spectrometer, recently proposed by Dr. Schnoepper, multiple photon thrusters and tethers are necessary for a pair of satellites to stabilize the angular disturbance.

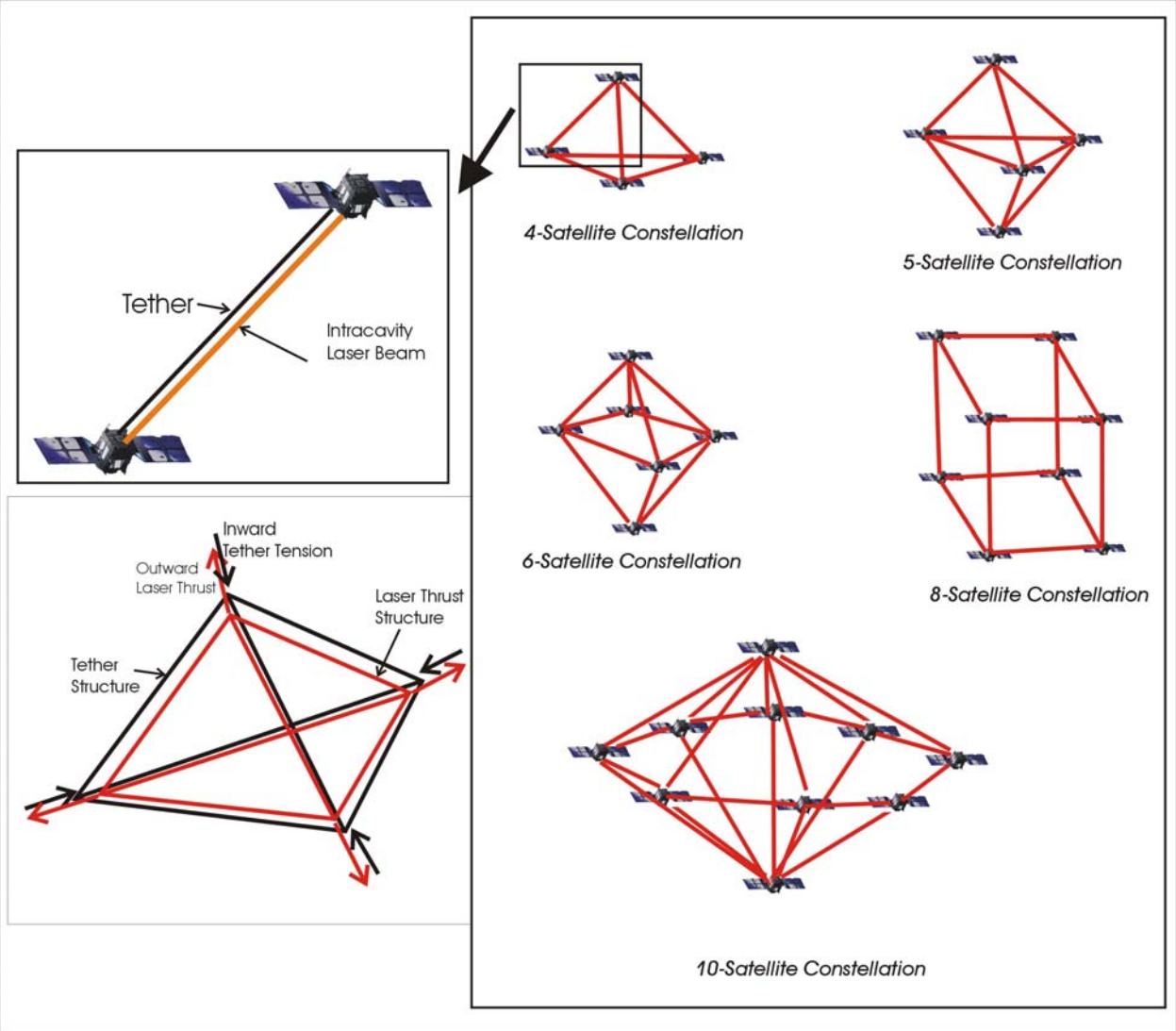

Figure 2. Schematic Diagrams of the Exemplary Satellite Mission Configurations with the Proposed Ultrahigh Precision Formation Flying Method. The 8-Satellite Constellation may require additional triangulation for stability.

More specifically, for SPECS applications, the proposed concept here has two important advantages. First, the usage of tethers will obviate the need for a massive amount of thruster propellant and high-quality imaging interferometry with a 1 km maximum baseline. "High quality imaging" implies the need for dense coverage of the "u-v" plane (i.e., moving the light collecting telescopes to fill the area subtended by the synthetic aperture). To produce images at a reasonable rate, the light collectors will have to be moved around a lot. Although even the most efficient thrusters available can't perform such a task, the tension in a tether can do nearly all the work. Second, to operate with the required sensitivity at far-IR wavelengths, SPECS will have cryogenic optics maintained at 4 K. Therefore, contamination of the optical surfaces is a big concern. The proposed system can be used as an alternative version for the originally proposed for SPECS to overcome these concerns.

The more detailed schematic diagram of the system architecture of the proposed system is shown in Fig. 3.

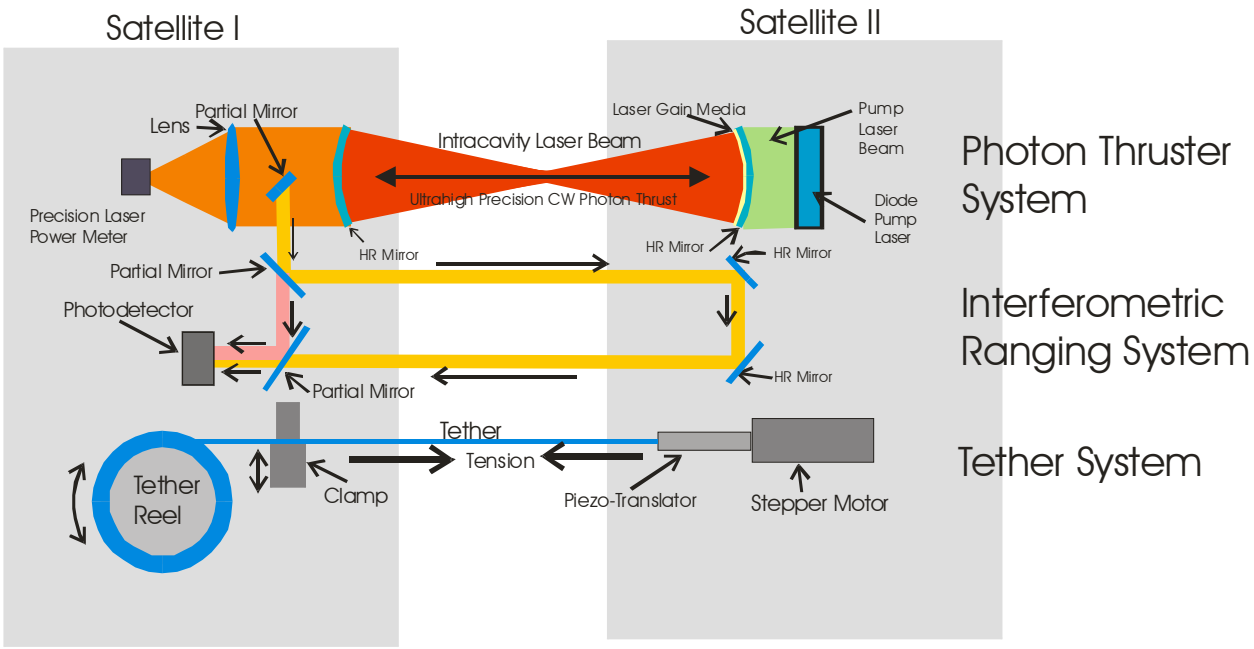

Figure 3. The schematic diagram of the combined system of photon thruster, interferometric ranging and tether systems. The electromechanical damper is configured with the tether clamp, and will be able to efficiently damp the transverse tether vibration efficiently.

The system has three major sub-systems: 1) the photon thruster system, 2) the interferometric ranging system, and 3) the tether system. The proposed ultrahigh

precision photon thruster will provide the thrust that will push the satellites apart resulting in extension as a function of the laser thrust. The opposite force is balanced by the tether tension and the length of the tether is proposed to be adjusted by linear translators composed of piezoelectric translators and stepper motors to the accuracy better than 1 nm. The ultrafine balance of the pulling-in and pushing-apart is maintained by the above two mechanisms and controlled by a computer in real time, forming crystal structure-like satellite cluster. The vibration perturbation or resonance induced by the actuation and motion of the systems and satellites in tether can be rapidly (almost in real time) damped by the photon thruster and electromechanical damper that is not shown in Fig. 3, but will be described in detail in the later sections.

For example, diode pumped solid state laser systems, such as a diode pumped YAG laser intracavity laser system, can be used for the proposed formation flying method. In this case, we estimate that the extracavity laser power in the order of 10 W capable of providing photon thrust up to mN is suitable for the weight of each satellite in the order of 100 kg. The power consumption and weight of such a laser system are estimated to be about 30 W and several kg, respectively. The intracavity laser beam is formed between two high reflectance (HR) mirrors located in two separate satellites. The matching tether diameter in this case, for example, is in the order of 4 mm with Kevlar fibers. The power of the laser and the inverse of the cross sectional area of the tether is linearly proportional to the weight of the satellite. For example, the formation of 10 kg and 1 kg satellite constellations, the required laser powers are in the order of 1 W and 0.1 W respectively. The weight of the laser system decreases rapidly as the laser power decreases, thus the technology can be easily adapted to much smaller and lighter satellite platforms. Eventually, the limiting factor in weigh scaling down will be the weight of the tethers and associated structures.

Another important issue that the effect results from that the spacecraft has size, moments of inertia, and attitude perturbation torques. Adjusting moving the tether attachment points may be the best way to get rid of steady-state "bias torques" on each spacecraft in an array, from weak environmental effects, or from the required transverse offset between the laser and the tether. Multi-element arrays don't need each connection to be torque-free, as long as all the connections on each spacecraft null out on the average. Periodic torques are easy to null out, with very small reaction wheels in each spacecraft.

In the following sections, the details of the subsystems of the proposed formation flying method are given.

B. Photon Thruster System

In this section the technical details of the intracavity photon thruster system shown in Fig. 4 are presented.

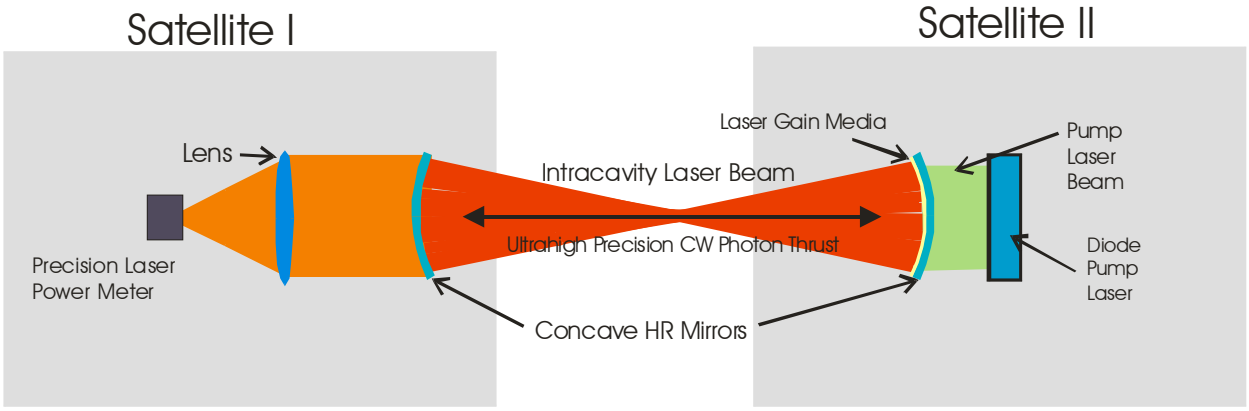

Figure 4. The schematic diagram of the photon thruster system.

The intracavity laser thruster system is proposed to be used to provide ultrahigh precision repulsive force between satellites against the tether contraction force. If the laser cavity is formed by two mirrors located separately in two satellites, the thrust, F_T, produced by a laser beam on each mirror is given by:

$$F_T = \frac{WRS}{c}, \tag{1}$$

where W the is laser power, c the light velocity, 3 x 10^8 m/s, R the reflectance, and S is the total power enhancement factor that is the ratio of the intracavity laser power to the extracavity laser power. Here, the preferred laser cavity is a confocal resonator that consists of two identical concave spherical mirrors separated by a distance equal to the radius of curvature of the mirrors. The usage of the confocal resonator is much more advantageous than that of a flat mirror resonator. The typical cavity with flat mirrors requires an angular alignment adjustment accuracy of the order of one arc second. However, the confocal resonator has a self-aligning property, thus the alignment requirement requires only about a quarter of a degree, two orders of magnitude less stringent than that with two plane mirrors. Furthermore, the former has much less diffraction loss than the latter (Fowles, 1975).

The total laser power in the intracavity is a function of the reflectance of the HR mirror and other complicated parameters, such as the saturation power of the laser media. Here we consider first the effect of the HR mirror reflectance. Because laser photons are virtually trapped in the intracavity laser formed between two mirrors, the average laser power in the intracavity will be amplified. If there is no saturation of the gain media and no thermal management limitations, the ideal total power enhancement factor, S, of the intracavity is given by:

$$S = \frac{T(1+R)}{(1-R)^2}, \tag{2}$$

where R is the reflectance of the mirror, T is the transmittance through the mirror given by 1 – R –A, and A is the absorption of the mirror coating during reflection. For high quality mirrors, A ~ 10^{-6}, thus, for the R < 0.99999, T ~ 1 – R, and the Equation (1) becomes:

$$F_T \approx \frac{2W}{(1-R)c}. \tag{3}$$

The parameters that determine the maximum attainable intracavity laser power are:

- The power saturation of the gain media
- The thermal management capacity of the gain media
- The HR mirror manufacturing consistency

For estimating the theoretical limit maximum intracavity laser power and the corresponding thrust, the other parameters are neglected, and results of the maximum theoretical thrusts as a function of the reflectance of the mirrors at the extracavity laser power of 10 W are summarized in Table 1.

TABLE 1. The Maximum Theoretical Thrusts of the Photon Thruster as a Function of the Mirror Reflectance at the Extracavity Laser Power of 10 W.

Maximum Operation Laser Power (extracavity)	HR Mirror Reflectance	Maximum Theoretical Thrust
10 W	0.90 - 0.99 (commonly used in laser cavities)	0.67 - 6.7 μN
10 W	0.9997 (Newport Supermirror)	220 μN
10 W	0.9999 (research grade)	0.67 mN
10 W	0.99995 (typically used super mirror)	1.34 mN

The optimum design of the proposed intracavity photon thruster is different from that of the typical laser cavities. The cavity design of the typical lasers is tailored to maximize the laser output power in the extracavity. Depending on the characteristics of the gain media, the reflectance of the output mirror (output coupler) is chosen 0.9 – 0.99 for the conventional laser cavities. In some cases the HR mirror with the reflectance of 0.999 has been used (Lee, 2005). To minimize the absorption loss in the gain media, the

proposed photon thruster should be designed to maximize the intracavity power, thus the gain media should be very thin to minimize the absorption loss in the gain media, similar to the one used in the state of the art solid state disk lasers used for intracavity second harmonic generation, except without the need of the frequency doubling crystal (Schielen, 2004). In this case, the thermal management of the gain media becomes an important issue.

In this analysis, we have only considered the reflectivity and absorption loss of the mirrors, however, several other factors including thermal limitation and optical absorption and saturation of the laser gain media have to be considered. In reality, because of the limitation in the laser gain medium and other thermal effect, the total thrust presented in Table 1 should be considered as upper bounds. The current off-the-shelf technological limit of the system reported to date is obtained with super mirrors used for the cavity ring down spectroscopy (Romanini, 1997) (currently available in the advanced research grade only) with the reflectance of 0.99995.

The maximum thrust of the proposed photon thruster as a function of the mirror reflectance, R, is shown in Fig. 5. Note that the x-axis represents 1/(1-R), which is approximately proportional to the number of reflections between two mirrors of the photon thruster. The photon thrust shown here is calculated for a 10 W laser system, and the higher laser power will reduce the required value for 1/(1-R) proportionally.

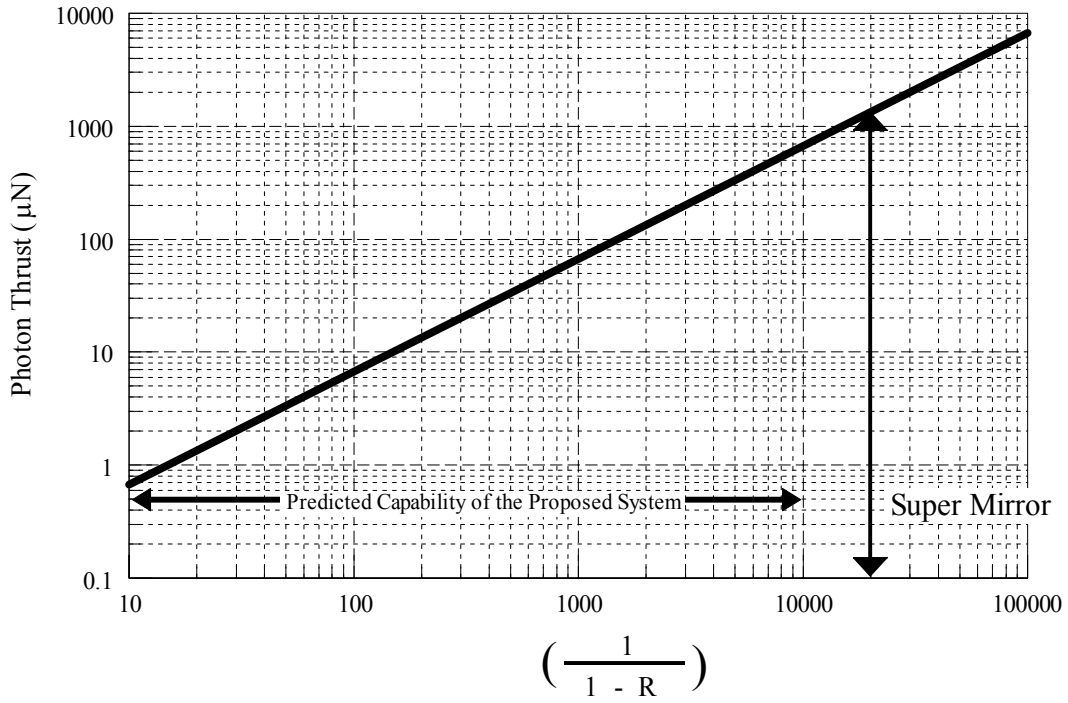

FIGURE 5. The Maximum Thrust of the Proposed Photon Thruster of 10 W as a Function of the Mirror Reflectance, R.

Based on the currently available laser technology, by making the gain media thin enough, the photon thruster with 0.999 -0.9999 is predicted to be readily possible with the laser design optimized for maximizing the intracavity power in the near future. With this, 10 W photon thrusters are predicted to be able to deliver up to 670 μN, which is large enough to compensate various perturbations in the space environment for most of missions envisioned as shown in Fig. 5. We note that the achievement of such high photon thrust will require highly sophisticated gain medium and pumping design and engineering, which is predicted to be within reach in the near future.

B.1. Photon Thruster Control Feedback Bandwidth

The proposed concept "inflates" and maintains the space structure using photons and tethers. Let us compare the proposed system with the one formed by gas inflated space structures that have been studied extensively and deployed in space. In the former structure, the photons are trapped by mirrors and the structure is constrained by tethers, while, in the latter structure membranes are used to both trap a gas and constrain the structural dimensions. The typical bandwidth of the control feedback of the structure depends on the medium that transmits the control. Because the photon velocity is much larger than that of sound velocity in the gas by about 6 orders of magnitude, the control feedback bandwidth of the former concept is much higher than that of the latter. In the intracavity arrangement of the photon thruster, however, the control feedback bandwidth can be much lower than that governed by the photon speed alone, because the cavity acts as a capacitor. The bandwidth in this case is proportional to the gain in the cavity. For example, with a gain of 10,000, the control feedback band width of the photon thruster concept is larger than that of the inflated membrane structure by only a factor of 100, which is still a very attractive figure. For the system that requires faster control response, therefore, the gain of the cavity is expected to be limited by the bandwidth factor.

B.2. Comparison of the Proposed Photon Thruster with other Microthrusters

We have investigated the detailed characteristics of the photon thrusters during this period in comparison with those of other conventional microthrusters. The reason that the photon thrusters have not been used is the thrust at a given propulsion energy is much smaller than conventional thrusters. The ratio of the thrust, T, to the propulsion power, P, is defined to be the specific thrust, T_S:

$$T_S = \frac{T}{P}. \tag{4}$$

For nonrelativistic case, $T = \dot{m}v$ and $P = \frac{1}{2}\dot{m}v^2$, thus $T_S = \frac{2}{v} = \frac{2}{I_{sp}g}$, where v is the exhaust velocity and I_{sp} is the specific impulse. For the photon case, $T = \frac{P}{c}$, thus $T_S = \frac{1}{c}$.

For both conventional thruster and the photon thruster, the specific thrust is inversely proportional to the I_{sp} or exhaust particle velocity; the higher I_{sp} the less is the specific thrust. Fig. 6 shows specific thrusts as functions of I_{sp} of various conventional and photon thrusters.

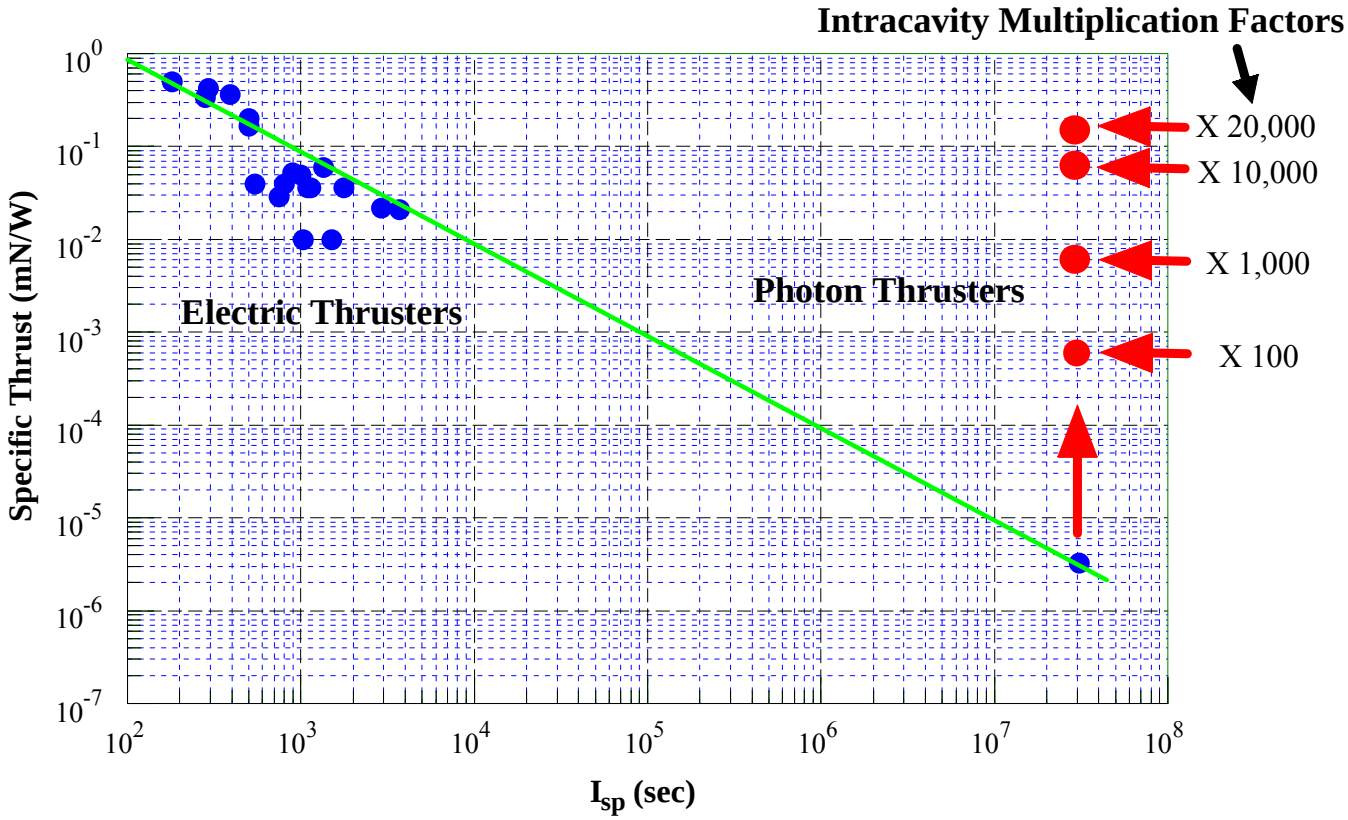

Figure 6. Specific thrusts as functions of I_{sp} of various conventional and photon thrusters. The specific thrust of the photon thruster without the intracavity momentum multiplication also follows the general trend of the most efficient electric thrusters, and is several orders of magnitude smaller than that of the electric thrusters with I_{sp} less than 10^4. However, with the intracavity multiplication factors greater than 1,000, the specific thrust of the photon thruster rivals that of the most efficient electric thrusters.

The specific thrust of the photon thruster without the intracavity arrangement is 4 – 5 orders of magnitude lower than the conventional electric thrusters as shown in Fig. 1, because of its high I_{sp}. Therefore, the regular photon thruster is highly inefficient in generating thrust, and this is the reason the photon thruster has been impractical in most of missions. However, with the intracavity arrangement proposed here, the momentum transfer, thus specific thrust, can be multiplied by "bouncing" photons between high reflectance mirrors. If the number of the reflection of photons is greater than 10,000, the specific thrust of the photon thruster becomes similar to the most efficient electrical thrusters as shown in Fig. 6. Most importantly, the proposed intracavity photon thrusters do not require rocket fuels, thus the mission Δv is not limited by the fuel capacity, but rather by the lifetime of the thruster, which is limited by the pumping diode lifetime.

B.3. Lifetime of the Photon Thruster

When the interferometer in the satellite cluster operates, the intracavity laser should operate continuously to dynamically adjust the relative distances and bearings between the satellites. The lifetime of the formation system is thus limited by the lifetime of the laser system. Currently, the lifetime of the diode pumped solid state lasers at full operation power is limited by that of pump diodes to about 10,000 hours (1 year) for continuous operation. With the reduced power operation or discontinuous operation the lifetime of the pump diodes is expected to be longer. In any case, the overall lifetime of the system can be further extended by simply replacing the pump diodes with new ones. The alignment of the pump diodes does not have to be precise; a design with carousels of pump diodes can be easily made. With a ten unit carousel, for example, the lifetime of the system is extended to tens of years. Moreover, with the rapidly developing diode laser technology, the lifetime is expected to increase significantly over the next decade. Therefore, the lifetime of tens of years of the photon thruster is well within the reach of the currently available off-the-shelf technology.

B.4. Maximum Range of Operation

The maximum range of the operation of the proposed system primarily limited by the diffraction limit of the intracavity laser, thus the diameter of mirrors. The theoretical limit of the intracavity length, L, for a confocal cavity resonator is given by (Yariv, 1975):

$$L = \frac{r_1 r_2}{\lambda} \quad , \tag{5}$$

where r_1 and r_2 are the radii of the laser beam projected on the mirrors, and λ is the wavelength of the laser. The required minimum diameter of mirrors for the photon thrusters as a function of the operation distance is given in Fig. 7.

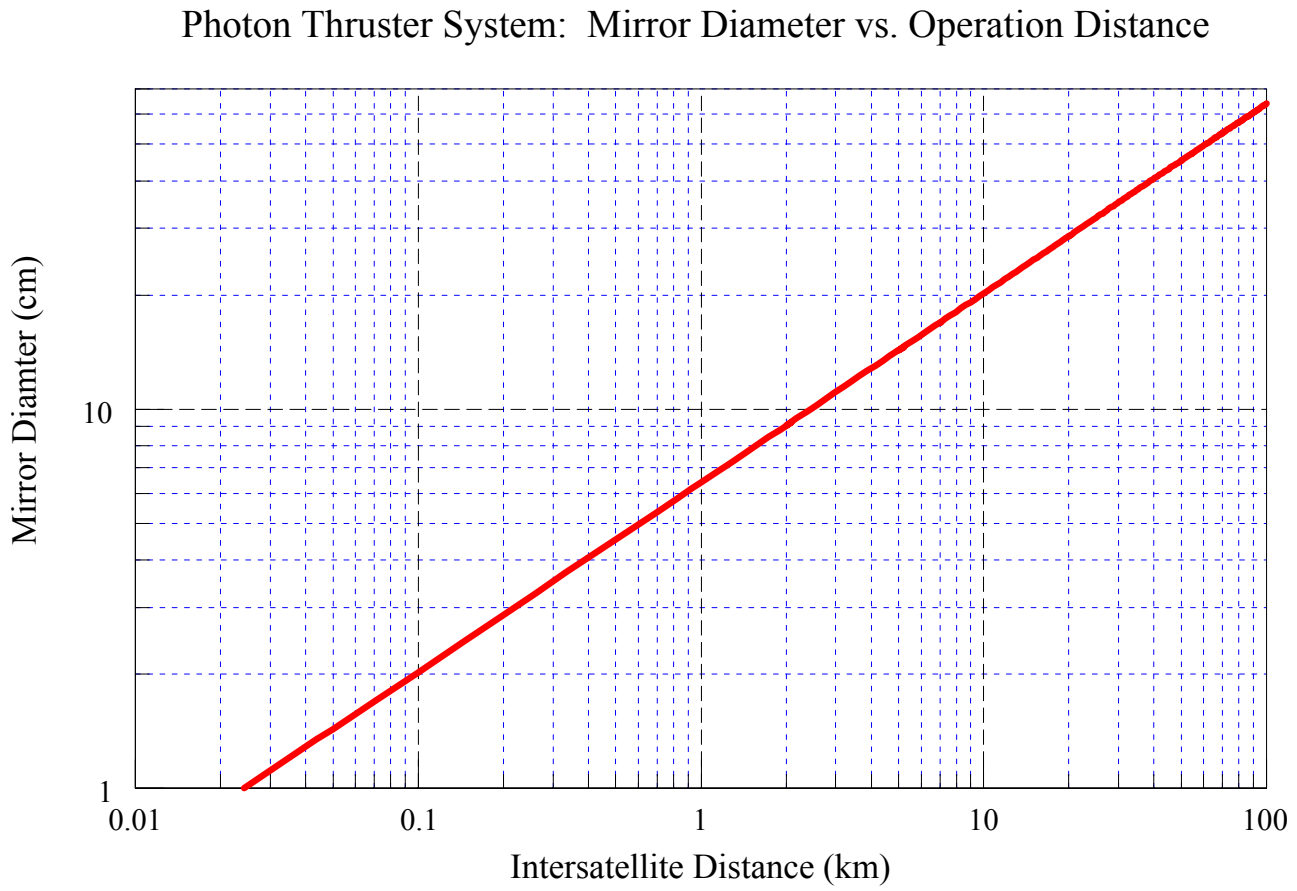

Figure 7. The required minimum diameter of mirrors for the photon thrusters as a function of the operation distance.

For example, for MAXIM applications with L=200 m, the required minimum diameter of the mirror is 3 cm. For the operation distances of 1 km and 10 km, the minimum diameters of the mirrors are 7 and 20 cm, respectively.

The diameter of the mirrors that can be carried by microsatellites and equivalent spacecrafts are probably limited by the weight of the mirrors. With the currently available technologies, the weight condition sets the limit on the mirror diameter to tens of cm. This in turn limits the maximum distance of operation to tens of km.

B.5. Deployment and u-v Plane Activity Related Issues

The deployment process of the proposed system can be achieved by firing the photon thruster at programmed thrust until the satellites establish a desired initial intersatellite distance, while the pointing/alignment of the laser is actively controlled by the mirror controlling system and the tether is gradually released. In the most of the envisioned missions, the need for dense coverage of the u-v plane requires continuously variable operation distance. In addition, in some missions, repeatable satellite segmentation and desegmentation may be necessary.

So far, we have considered the design and performance of the proposed system at the maximum intersatellite operation distance. Because the curvature and radius of the mirrors of the proposed formation flying method are designed for the maximum baseline distance, during deployment process and u-v plan activities at shorter distances, the laser beam in the cavity will be defocused. In this case, the characteristics of the laser cavity will be in between that of the confocal cavity and that of the flat mirror cavity. The fractional power loss per transit of the laser beam in the intracavity is a function of the Fresnel number, N given by (Fowles, 1975):

$$N = \frac{r_1 r_2}{\lambda L} \tag{6}$$

where L is the length of the laser cavity, r_1 and r_2 are the radii of the laser beam projected on the mirrors, and λ is the wavelength of the laser. In the proposed system, r_1, r_2 and λ are constant, thus N is inversely proportional to L. The fractional power loss per transit is a function of N, and for the confocal cavity, it is a rapidly exponentially decreasing function of N, while for the flat mirror cavity, it is a slowly exponentially decreasing function of N (Fowles, 1975). At shorter operation distances, as N increases, the curve of the fractional power loss per transit shift from that of the confocal cavity to that of the flat cavity. At very short operation distances, particularly during the initial deployment, the laser cavity is close to that formed by flat mirrors. These effects of increased N and the shift of curves on the fractional power loss per transit in the laser cavity are expected to compensate each other; however, the degree of compensation is not known currently. If the effect of the increased N on the fractional power loss per transit under-compensates that of the curve shift, the increase of the mirror diameter is necessary. The details of the optical analysis of these issues will be performed in Phase II.

B.6. Photon Thruster Intracavity Mirror Alignment Issue

The laser system alignment at the onset of deployment is straightforward, because of the proximity of the satellite will result in a large solid angle projected by the opposite mirror. As the formation structure is inflated, the jittering of satellite positions may result

in misalignment of the laser cavity. Therefore, the laser mirrors have to be actively aligned as the cavity length increases during initial deployment stage. This active alignment can be performed with piezo-crystals attached to the mirrors. The control of the piezo-crystals will be achieved by active feedback signals from the photon detectors, for example, four photo detectors covering four quadrants as shown in Fig. 8.

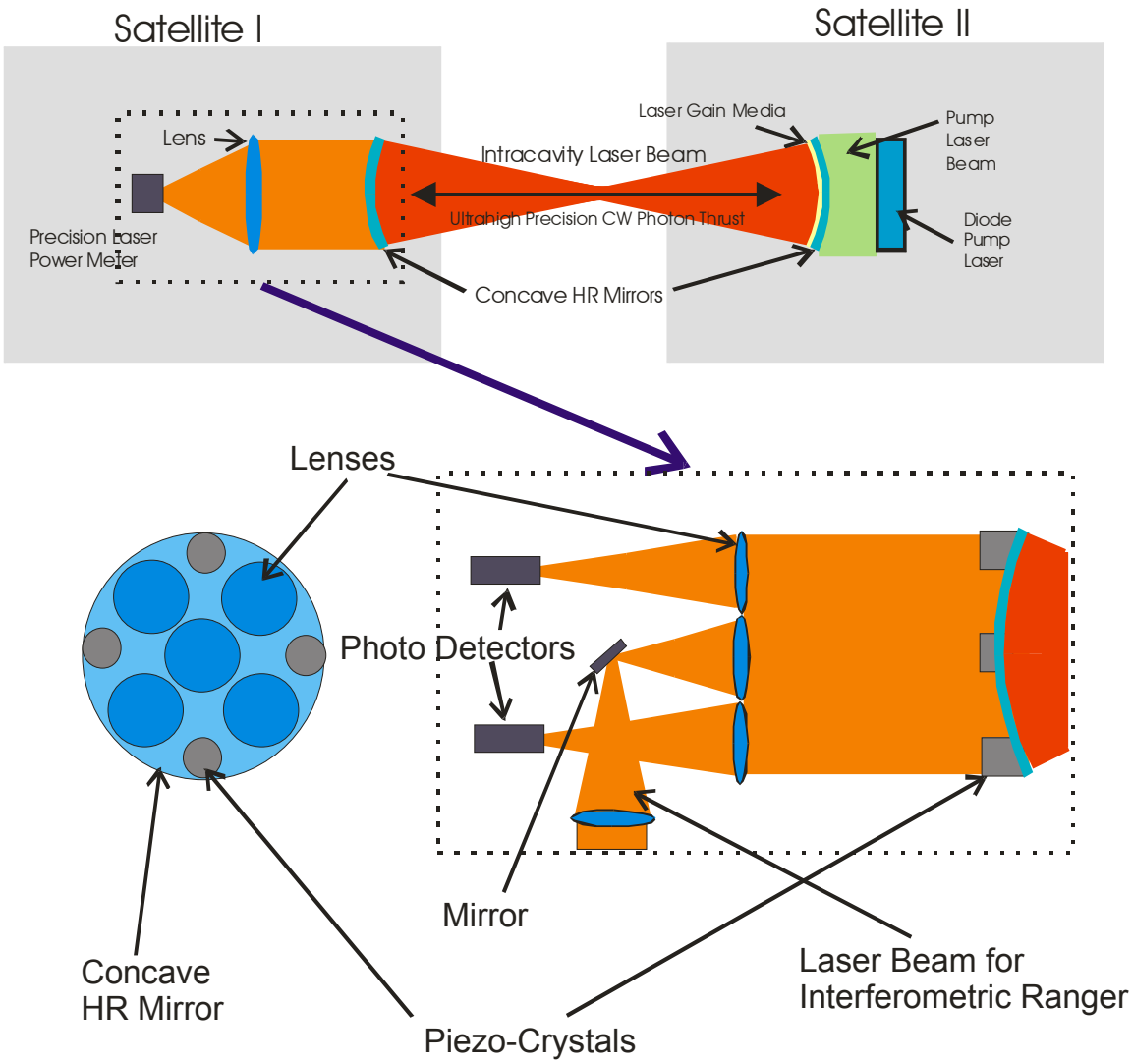

Figure 8. Schematic diagram of the HR laser mirror alignment system showing the details of subsystems, including four quadrant photo detectors and lenses, piezo-crystals, and a laser beam split for nano meter precision interferometric ranging system described in the next section. The piezo-crystals align the HR mirror based on the feedback signals from the four quadrant photo detector outputs.

However, after full deployment and during operation, if the alignment of the laser is lost due to some major perturbations, including micrometeoroid impact, the reestablishment of the laser cavity locking may be a non-trivial issue. In this case, the typical laboratory procedure for establishing initial laser beams: rocking or scanning the mirror alignment until the lasing starts. Once the onset of lasing is detected, the alignment mechanism will tune or maximize the laser power and quality.

C. Interferometric Ranging System Integrated with Photon Thruster System

In the conventional formation flying control, each spacecraft has to equip with both lateral and longitudinal control systems including thrusters and metrology systems. The use of crystalline structure in the formation flying simplifies the formation control, and only longitudinal control and metrology systems are necessary. Furthermore, our innovative design concept simplifies the system further by combining the propulsion systems and metrology systems together.

The precision formation flying of satellites will require a highly sophisticated ranging system for monitoring the intersatellite distance for the next generation NASA missions. If the thrust of satellite maneuvering is provided by conventional microthrusters, the ranging will require additional laser based interferometric system to the thruster control system. The proposed formation flying method takes advantage of the dual usage of the photon thruster as a laser source of the interferometric ranging system. This is possible because in operation the intracavity laser of the photon thruster will be operated with high stability ideal for the ultrahigh precision interferometric ranging application. The proposed dual usage will significantly simplify the system design and reduce the system weight and power consumption.

We have investigated the optimum way of combining the interferometric ranging system with the photon thruster system. One of the best candidates for the ranging system for the proposed ultrahigh precision formation flying method is the laser interferometric ranging system. (Jeganathan, 2000, and Bender, 2003) Fig. 8 illustrates the schematic diagram of the proposed subsystem with a Michelson interferometric scheme in which a portion of the extracavity laser beam is reflected by a partially reflecting mirror (or a fully reflecting mirror) to be used for interferometric ranging. The schematic diagram in Fig. 9 represents one of many possible designs, and the selection of the most suitable system may depend on the specific mission requirement. The interference of the primary laser beam in the primary satellite and the laser beam reflected by the mirrors in the secondary satellite is used for assessing the relative distance change between the satellites. This Michelson interferometry design of the ranging system is relatively straightforward, but the ranging accuracy is in the order of tens of nms. The nm

accuracy ranging will require more sophisticated interferometric ranging system that will be discussed below.

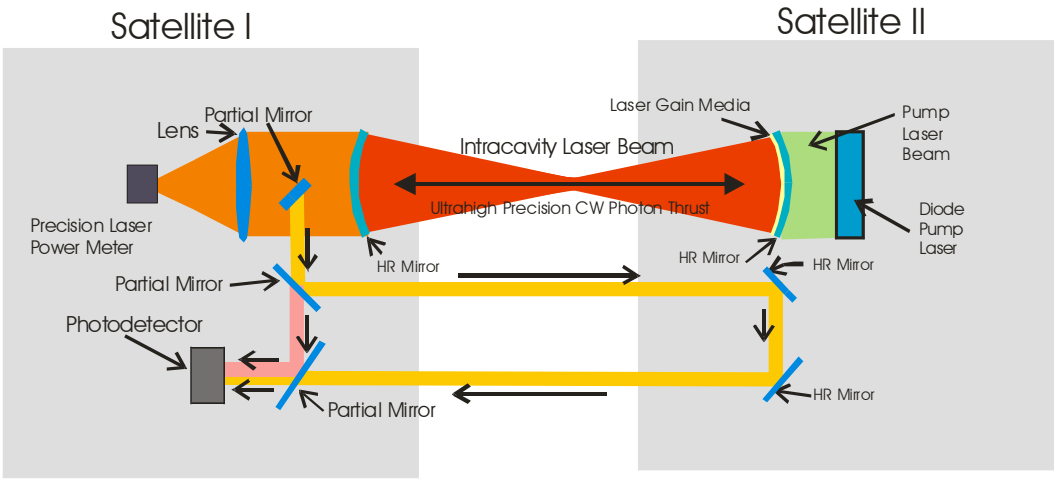

Figure 9. Schematic diagram of the photon thruster coupled with the laser interferometric ranging system. Because of the dual usage of the photon thruster laser for the interferometric laser, the system configuration and control becomes simplified with reduced mass and cost.

During operation, the power of the photon thruster will be maintained ultrastable and the force fluctuation due to the environmental perturbation will be countered by varying the tension of the tethers with the precision translators. Upon encountering large environmental perturbation or major realignment of the whole formation structure, the tether vibration will be generated. The details of tether vibration countering scheme will be extensively discussed in the later sections. The rapid countering of longitudinal tether vibration can be achieved by modulating the laser power. Even in this case, the interferometric ranging system can be designed to be insensitive to the overall laser power fluctuations, because its operation relies on counting the interferometric fringes rather than measuring the absolute power measuring. The more technical details of this scheme are of Phase II topics.

The requirement for the absolute longitudinal metrology depends on missions, and will not be considered in this report. In any case, it is highly technically challenge for the design to achieve nm accuracy. Heterodyne interferometry is based on the production of two coherent beams; a reference and a measurement beam with slightly different frequencies. This can be done with two lasers or one laser with two acousto-optical modulators (AOM). To simplify the architecture, we have chosen the latter design. The schematic diagram of the proposed heterodyne interferometric metrology system in combination with the photon thruster system is shown in Fig. 10.

In the proposed design, the first parts of these beams are sent to the reference detector in which they interfere. The second part of the beams are sent to a reference retroreflector and sent back to the measurement detector. The second par of the

measurement beam is sent to the target retroreflector and is then sent back to the measurement detector in which it interferes with the reference beam. The phase difference between the signal on the two detectors, which is proportional to the path difference, is transformed from the optical frequency region into an electrical one, and the phase differences are measured. With the reference system located in the satellite II and the measurement system located at the satellite I, using a return beam between these satellites the relative distance variation can be measured to nm accuracy.

The present method represents one of many possible designs, and the selection of the most suitable system may depend on the specific mission requirement. One of the concerns is the possible interference between the two systems. During operation, the power of the photon thruster will vary to counter the intersatellite distance change resulted from the environmental force perturbation. However, the interferometric ranging system is not sensitive to the overall laser power fluctuations, because its operation relies on counting the interferometric fringes rather than measuring the absolute power. Therefore, the possibility of interference between the two systems is minimal.

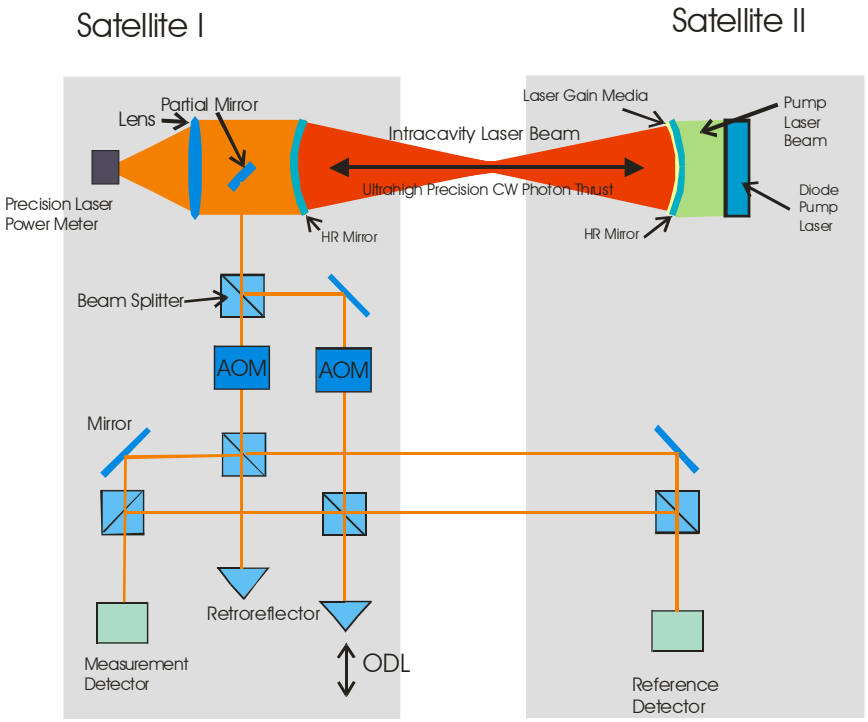

Figure 10. Schematic diagram of the photon thruster coupled with the improved heterodyne laser interferometric ranging system capable of measuring the distance to nm accuracy. Because of the dual usage of the photon thruster laser for the interferometric laser, the system configuration and control becomes simplified with reduced mass and cost. AOM: Acousto Optical Modulator. ODL: Optical Delay Line.

D. Tether System

D.1 Overview of the Tether System

The proposed intracavity laser system will be combined with a tether system that will provide pulling-in force between a satellite pair through tension. For the gross length adjustments of the tether, in one of the pair satellite is proposed to have a reel mechanism and inchworm actuator that can be clamped to or released from the tether to allow low-noise fine adjustments (Fig. 11).

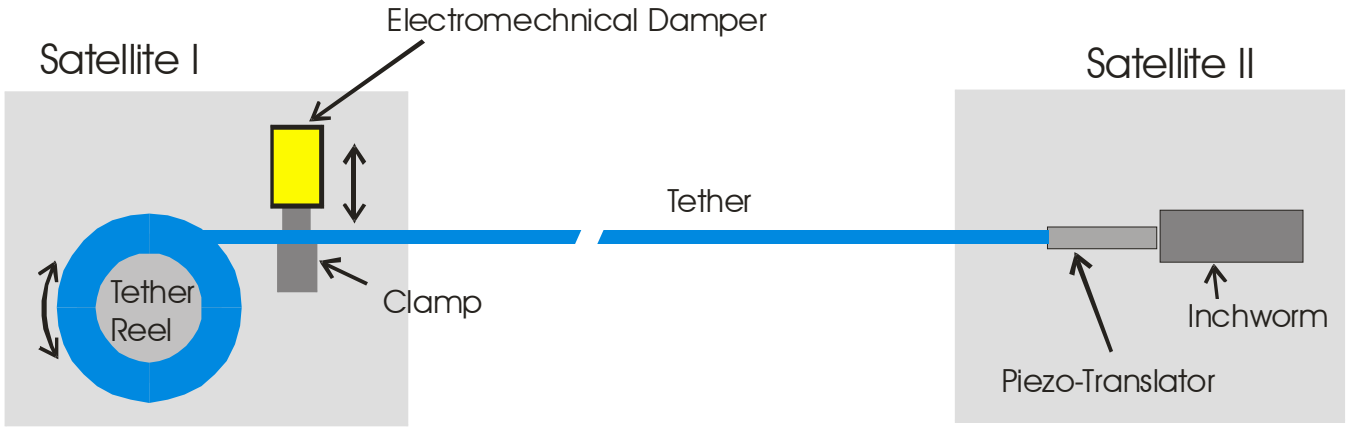

Figure 11. The schematic diagram of the tether system.

The tether will be extended with the use of laser thrust that will be counterbalanced by the tether tension. The other satellite in the pair is proposed to have a piezoelectric translator with sub nm accuracy. Currently, off-the-shelf commercial piezoelectric translator can deliver the accuracy resolution of 0.02 nm. Because the accuracy in the distance maintenance relies on that of the piezoelectric translator, the proposed system will be able to deliver the sub nm accuracy.

Let's consider a 1-D system that consists of two spacecrafts connected with a tether. In this case, the variation in length Δl_F with the tension F_T, which is counterbalanced by laser thrust, is given by:

$$\Delta l_F = \frac{1}{Y}\frac{F_T}{A} l \,, \tag{7}$$

where Y is the Young's modulus, A is the cross sectional area of the tether, and *l* is the length of the tether. This can be rewritten as a Hooke's law type equation:

$$F_T = k\Delta l_F \tag{8}$$

where $k = \frac{YA}{l}$.

If the tether is stretched by the photon thrust force, F_L, the total force, F, applied on the tether, thus spacecrafts, is given by:

for x>0,

$$F = kx - F_L + F_P \tag{9}$$

and for x<0,

$$F = -F_L + F_P . \tag{10}$$

Where $x = \Delta l_V$ and F_P is the equilibrium force on the spacecrafts from the environmental perturbation, such as gravitational gradient and solar pressure. In the normal operation, by stretching the tether with the photon thruster force $F_L > F_p$, the system operation will be limited for the case x>0.

D.2. Nano-Meter Accuracy Baseline Control

F_P can be countered by controlling either the photon thruster force, F_L, thus the laser power thrust, or the length of the tether. In the case in which F_P is countered by controlling F_L, the tether length is kept constant by controlling the pump diode laser power with the feedback distance signal from the laser ranging system. The finesse of the distance accuracy in this case comes from the ability of fine tuning of the laser power and stability. We consider a system that has 1 km baseline distance, thus a 1 km Kevlar tether with a diameter of 4 mm. In this case, $Y=10^{11}$ Pa, and $k = 1.2 \times 10^3$ N/m. For the change of the distance of 1 nm, the photon thruster accuracy should be 1.2×10^{-6} N = 1.2 μN. For example, for L2 orbit applications, F_P is estimated to be less than 50 μN, and the average F_L will be maintained around 100 μN, which will stretch the tether by 90 nm. Therefore, the required thrust accuracy is 1.2 %, which is well within the reach of the off-the-shelf laser power accuracy.

Another way to maintain the interspacecraft distance with 1 nm accuracy in the above example is that the tether is stretched by the constant photon thrust of 100 μN in average, and the perturbative force is counter balanced by changing the tether tension by moving the piezoelectric translators. In this case, because the piezoelectric translators have the resolution much better than 1 nm, the limiting step is the photon thruster power accuracy, and to obtain 1-nm accuracy, the photon thrusters should have

the noise to main power ratio in the order of 10^{-2}. In the currently available CW laser systems, the noise to main power ratio of 10^{-5} can be achieved. Theoretically, the piezoelectric translator can be continuously controlled in real time by the feedback distance signal from the laser interferometers that measure and monitor the intersatellite distance continuously. Therefore, the proposed intracavity thruster system, in principle, can provide the distance adjustment better than nanometer accuracy.

D.3. Tether Vibration Control

The proposed PTFF will be cable of providing near adiabatic CW position control of spacecrafts, thus the photon thruster and tether control system will generate minimal abrupt perturbation unlike the control system with conventional microthrusters that will provide typically pulsed impulse bits. However, there are several other mechanisms that may cause significant perturbations on the dynamics:

1) If a tether is highly loaded, and some filaments break, the result will be a "step function" relaxation, followed by ringing.

2) A small micrometeoroid or debris strike to a tether will also break some strands, and causes a step change plus ringing that will travel back and forth on the tether until it is damped out.

3) Major reorientation of the whole formation structure.

Because the damping process will result in deadband situations and significant consumption of the system power, one of the aspects of the PTFF dynamics is what can excite and how one can damp these modes, in particular with the use of computer simulation. Numerous excitation modes of tethers are anticipated in tethers connecting both orbiting or stationary satellites/spacecraft in formation flying. These modes can be classified into 4 major types:

1. Low-frequency tether bending modes
2. Medium-frequency "sprung mass" modes (ignoring the mass of the tether itself)
3. High-frequency "taut string telephone" axial modes
4. Tethered end-mass attitude motion.

In orbiting tethers, the lowest frequencies are typically associated with libration. Libration is likely to be of concern mostly not from the point of view of dynamics but from the constraints that gravity gradient torques impose on the pointing of interferometers and similar instruments. (That will require study, but it is distinct from the dynamics issues that are being addressed here.) Low-amplitude libration has a period of 0.577 orbit for in-plane swings and 0.5 orbit for out-of-plane dynamics. This is ~1 hour in LEO, or ~6 months in heliocentric orbit. Somewhat faster (typically 1-10

minutes in LEO, depending on the tether length and the ratio of tether mass to payload mass) are the transverse modes of the tether. Faster yet is the typical "fundamental sprung-mass" mode, with the tether serving as a long, low-cross-sectional-area, low-spring-rate, nearly-massless spring between two endmasses.

The highest frequencies associated with the tether itself are typically the string axial modes, in which the tether acts like the taut string telephone that most children have played with. Typical high-strength non-metallic tethers like Kevlar, Vectran, or Spectra have sound speeds of 5-8 km/sec, so the lowest such frequency is typically a second or less. Much higher frequencies are also possible. In the limiting case, nearly "square wave" tension profiles can propagate along the tether, and reflect back and forth between the ends. In a vacuum environment, damping is limited to that intrinsic to the tether or provided by the end attachments or endmasses. If a tether is highly loaded, and some filaments break, the result will be a "step function" relaxation, followed by ringing. A small micrometeoroid or debris strike to a tether will also break some strands, and causes a step change plus ringing that will travel back and forth on the tether until it is damped out.

Efficient and realistic simulation of tether dynamics in space has been a daunting task. The main idiosyncrasy of simulation of tethered systems is their "computational stiffness." This refers to a radical difference between the highest and lowest relevant frequencies in the system. This problem also occurs in other physical systems. One is detailed simulation of electrons and ions in plasmas, due to the mass difference. Another is simulation of the evolution of galaxies, due to the time-scale difference of individual star motions vs the slow evolution of the massive core. Stiff systems are computationally demanding, because you need short timesteps to do justice to the high-frequency dynamics, but you need long simulations to see the effects of the low-frequency modes.

Tether dynamics specialists have written a variety of simulation programs. Even the same analyst will often write different programs to study different aspects of the dynamics. Since the tether excitation frequencies are so far apart, the dynamics and control for each of them can be studied somewhat independently to the first order approximation. However, a systems perspective is needed to ensure that the "fix" for one type of dynamics does not become a strong driver for disturbances of another type. This will require a combination of analysis and simulation. This "integration" effort might use a detailed existing simulation tool that is computationally too intensive for most of the detailed studies. For example, Dave Lang's "GTOSS" (Generalized Tethered Object Simulation System) may be appropriate for studying interactions between modes. But note that GTOSS tends to run slower on a Cray than TAI's "BeadSim" program does on a PC. (In cases studied at JSC, both programs gave similar results.) BeadSim speeds up calculations by artificially damping the taut-string telephone modes rather than keeping track of them. This is justified during SEDS deployment, but not for many other cases. TAI has also written a "1-D" simulation program to simulate the axial response of a long (even tapered) tether to capture or

release of end-masses, with or without reeling. This model handles the taut-string telephone modes that BeadSim cancels, and deals with damping in an explicit manner. As with nearly all models, the model does include some artificial damping that is intrinsic to the discretization part of modeling. But that artificial damping can be quantified and compensated for by adjusting the explicit damping model.

There are three areas that will require particular care in this modeling effort. One is modeling the weak environmental effects that can drive the dynamics. This includes both "fast" effects like micrometeoroid impact, or slippage at the attachment points, and also "slow effects" such as temperature changes with orientation. The issue is to determine which of many very weak forces might be of most concern. This is likely to require a combination of analytical and simulation work.

A second area is appropriately modeling the tether attachments, and any control capabilities built into them. It seems likely that in many applications, one will want to change the baseline length by significant amounts. This requires reeling, which will probably be quite noisy (on the scale relevant to interferometry). It will be followed by periods of "quieting the system down." We suspect that during non-reeling times, one will want to actively clamp the tether, to prevent slippage on the reel or any drive pulleys, and the resultant noise from such slippage. But such attachments are not likely to have much damping. Hence one may want to add a piezo-electric or other actuator into the clamp support, to provide agile short-stroke control to damp out the residual high-frequency dynamics. We have been searching for the most suitable satellite simulation program for testing the proposed concept. Currently, most of commercially available simulation programs are not equipped with the tether dynamics.

The third area is about the appropriate division of labor between such a mechanical actuator, and a photon thruster actuator. The piezo-electric actuator will take less power and mass for a given force, but it will have a slower response than the laser (especially at the far end). In addition, it cannot provide a separation force, as the photon thruster can.

The proposed ultrahigh precision formation flying, therefore, needs the ability to damp out tether vibrations generated by maneuvers and environmental perturbations. For simplicity, in this report, we only consider two major types of tether vibrations that are expected to be generated: longitudinal and transverse vibrations. More detailed tether vibration studies will be undertaken in Phase II.

In general, longitudinal tether waves are readily damped by the tether material friction and, if necessary, by modulating the laser power in the photon thruster. Transverse vibrations that are typically excited by retargeting maneuvers can be damped out by vibration dampers located near the attachment points of the tethers to the spacecraft. We propose to use an electromagnetic damper incorporated into the tether clamp system as shown in Fig. 9. In this conceptual design, the clamp acts as an impedance coupling mass and the linear motion induced by the transverse tether vibration is

coupled through an electromechanical shock-absorber-like damper. In this damping mechanism, the linear motion stiffness and damping can be adjusted by changing electrical parameters over a wide range.

The transfer of energy carried by the waves from the tether to the passive damper is maximized when the tether wave impedance is matched to the damper impedance Miller and Hall, 1991). The impedance of transverse tether waves, Z_1, is given by

$$Z_1 = \mu v \tag{11}$$

where v = $(T/\mu)^{1/2}$ is the wave propagation velocity, T the tether tension, and μ the tether linear density. The impedance, Z_2, of the damper responding at the wave angular frequency ω is given by

$$Z_2 = d + i\left(m\omega - \frac{k}{\omega}\right) \tag{12}$$

where *m, d,* and *k* are the mass of the damper, damping coefficient, and spring constant, respectively. By equating Z_1 and Z_2 one obtains the results: (a) d=μ v, and (b) $\omega = \omega_0 = (k/m)^{1/2}$.

The wave transmissibility function (Pain et al. 1983) has the same formulation of the energy loss per damping cycle of waves propagating along a tether terminated with a spring and dashpot massive damper, as computed in Beletsky and Levin (1993). Fig. 12 shows the fractional reduction of the wave amplitude per damping cycle (δA/A), derived from the wave transmissibility function, for cases of maximum and minimum baseline lengths of the formation flying structure (Lorenzini, Bombardelli, and Quadrelli (2001)). Note also that the tangential velocity of the collector spacecraft (with respect to the system center of mass) was assumed equal to 2 m/s and 0.05 m/s at the maximum and minimum baselines, respectively, in order to maintain the angular rotation rate of the interferometer approximately constant during an observation, as currently planned.

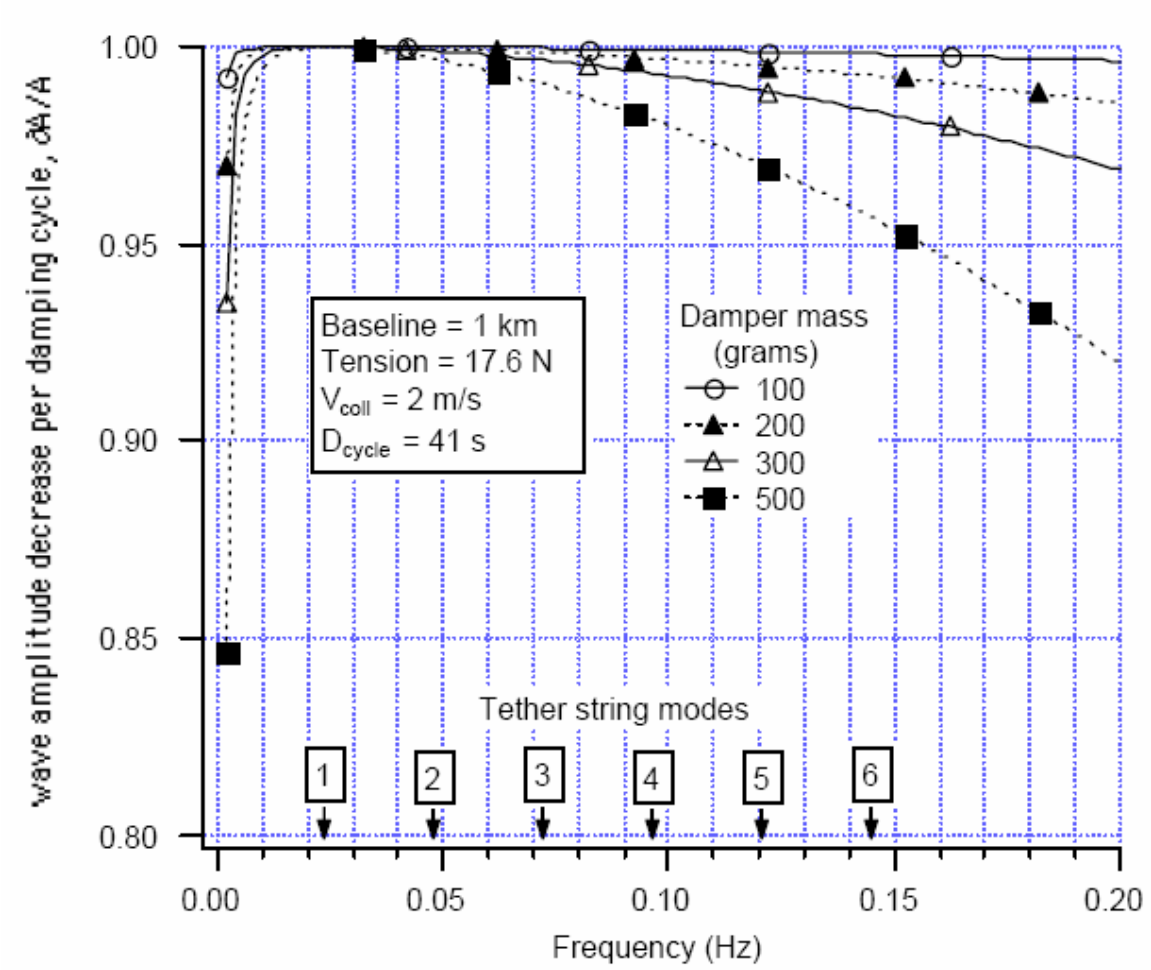

Figure 12. Wave amplitude reduction per damping cycle vs. wave frequency for different masses of the tether attachment point damper at the baseline length of 1 km and collector's tangential velocity of 2 m/s. From Lorenzini, Bombardelli, and Quadrelli (2001).

The result in Fig. 10 shows that if the damper is tuned to the first modal frequency of the transverse waves, the first mode is damped in one damping cycle *(D_{cycle})*. However, higher frequency modes take more than one cycle to damp out, but a damper with light mass can damp very effectively higher-order modes over a few damping cycles, especially at long baseline lengths. The analytical results were confirmed through numerical dynamics simulations by Lorenzini, Bombardelli, and Quadrelli (2001) of the interferometer at a 1-km baseline. Their result presented in Fig. 13 shows the transverse oscillation amplitude, measured at the tether mid point after a quick (and consequently perturbative) retargeting maneuver. The impedance-matched damping system that is activated at t = 4,000 s rapidly abates the lateral oscillations as predicted.

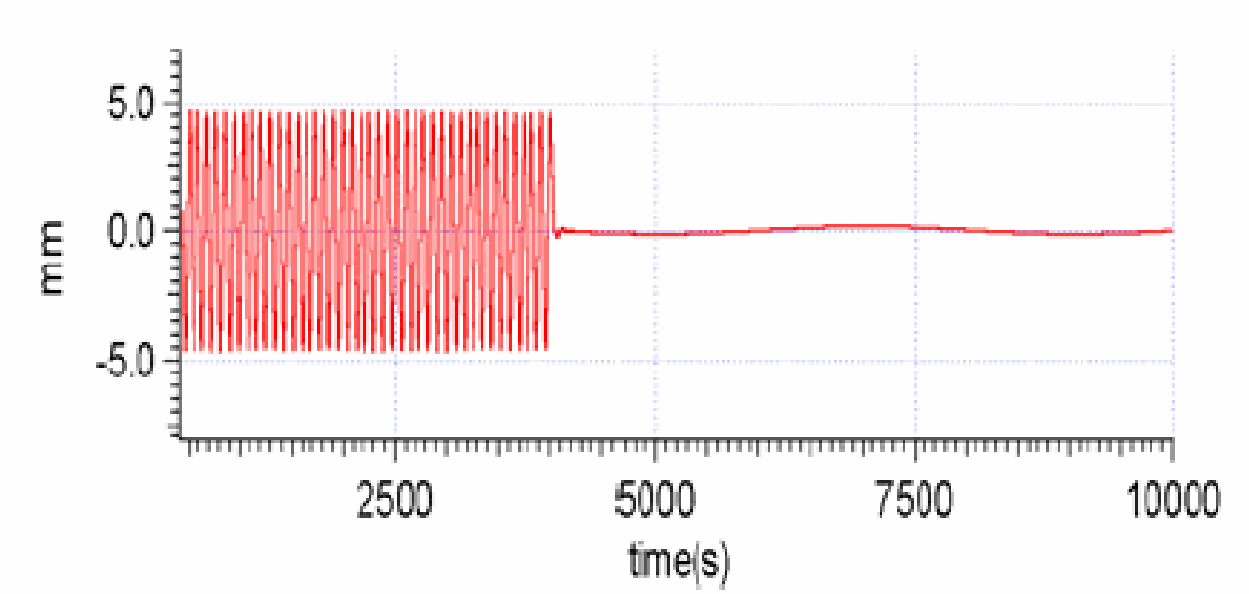

Figure 13. Tether transverse vibration damping from numerical simulations on the mid-point tether amplitude. From Lorenzini, Bombardelli, and Quadrelli (2001). Note that the vibration did not decay even 4,000 sec after the tether excitation. However, the impedance-matched damping system that is activated at t = 4,000 s rapidly abates the vibration.

D.4. Thermal Contraction/Expansion of the Tether System

One of important problems that the tether based system will encounter is thermal expansion/contraction of the tethers due to exposure or non-exposure of sunlight. In fact, this thermal expansion/contraction is the key factor that limits the usage of any formation methods relying on solid monolithic structured beds, in which the engineering of the real-time response system to the thermal effect is daunting. However, the proposed system with tethers and photon thrusters has a built-in capability of responding to such thermal perturbation. In the proposed tether system, the length change Δl_t resulted from the temperature change Δt is given by:

$$\Delta l_t = \beta l \Delta t \,. \tag{13}$$

For example, at l = 1 km an environmental temperature change, Δt =10 C, will result in the tether length change as much as 5.5 mm. Because the thermal perturbation will be a very slow process (matter of hours or even days), it will be readily compensated by a piezoelectric linear translator coupled to the tether in the similar fashion to the force perturbation. The interferometer monitors the change and provides the feedback signal that controls the piezoelectric translator for compensation. If the temperature change results in the tether length changes greater than the dynamic range of the piezoelectric

translator, a reel and/or stepper motor system will kick in to provide much larger dynamic range.

D.5. Tether Lifetime Issue

The lifetime of the tether in the space environment is a critical limiting factor on the lifetime of the mission with PTFF. For example, risk of tethers being cut by micrometeoroids or orbiting man-made debris is an important issue for tethered systems operating in LEO. Currently, experimental data on the rate of failure of a tether line is limited to the results of the SEDS-2 experiment and the TiPS experiment in LEO. Thus, it is not possible to assess the breakdown of the tether used in operations in other orbits, such as MEO, LEO, and Lagrangian Orbit. In general, the lifetime in LEO can be considered to be the lower bound for the lifetime in other orbits, thus, in this report the breakdown of tethers in LEO operation is analyzed.

The micrometeoroid and debris risks vary differently with tether diameter. Debris is the dominant risk for large tethers (>3 mm) at LEO altitudes above 400-500 km, on the other hand, micrometeoroids are for thinner tethers or lower altitudes. There are wide ranges in estimates of tether risk. One approach is based on **SEDS-2** experience. The 19.7 km long **SEDS-2** tether was cut 3.7 days after deployment, and the remaining 7.2 km length appeared to remain intact for the remaining 54 observable days of its orbit life. This means there was 1 cut in 460 observable km-days of exposure of a 0.78 mm diameter braided Spectra tether. Carroll and Oldson, [13] extrapolated the SEDS-2 data to other sizes by scaling with crater size distribution data derived from LDEF and other sources. The results fit the following simple expression:

$$\text{Estimated MTBF} = (D_t + 0.3)^3, \tag{14}$$

where the Mean Time Before Failure is in km-years and the tether diameter D_t is in mm. This is the only available unbiased flight-based estimate of tether MTBF at present. The actual MTBF could be much higher or lower. The above formula predicts that a 1 km tether with a diameter of 1 mm has a lifetime 2.2 years, and a 4 mm tether 80 years.

The tether lifetime in other orbits is expected to be much longer, although there is not enough technical data to estimate it accurately. Furthermore, the perturbation force is expected to be much smaller, thus the system requirement should be much more relaxed than that of the LEO operation. During Phase II, this aspect will be investigated further.

D.6. Nonlinearity of Tether Properties

Tethers have distinctly non-linear and non-ideal behavior at very low tension, in particular in the mN range. A tether of order mm thick (thick enough to have a decent probability of survival), or some kind of collection of narrower tethers with cross-links (caduceus, Hoytether, or other), will both have distinctly non-Hooke's-law stress-strain response at millinewton-level tensions. In this case, the effective modulus may be orders of magnitude less than that at higher tension, because at low tension, most of the strain associated with changes in that low tension is due to residual straightening of the bulk tether and of the fibers that make it up. And that behavior will change with temperature, time, and handling history.

The short-term predictability and hence the controllability proposed here may be adequate, but modulus values may not be representative of lines that are under enough tension to be nearly straight. It may be important during initial deployment (or after unwinding tether to increase spacecraft separation in an array) to cause some sort of brief tension spike that is long enough to get rid of the worst of the "curvature memory" but without causing much acceleration of the spacecraft that would be hard for the lasers to cancel out. Or it may be enough to pass the tether through a series of "straightening rollers" after it comes off the storage spool, to minimize memory of curvature. Overall, this aspect is of minor concern, and during Phase II, this issue will be addressed in detail.

D.7. Ideal Tether for PTFF

The ideal tether for PTFF does not need much strength, but it needs environmental resistance, including impact resistance to micrometeoroids. Spectra (or its European equivalent, Dyneema) tethers they have the best impact resistance, however, one could use nylon, if lower stiffness seems to work better, and if the nylon can hold up in vacuum ultraviolet as well as polyethylene does. As far as tether constructions, there are several property parameters that can be adjusted, which might have some effect. .One parameter is choosing between hollow tubular braids and flat braids (with several complete twists from end to end, so minor twist variations don't cause significant changes in solar pressure). One could even go to a twisted-strand "thread-like" construction, but I'm not sure that would be an improvement. If flat braids are used, another adjustable parameter is the amount of twist put into the completed braid. We don't want enough to significantly torque the endmasses, but we need some twist to null out variations in solar pressure forces on the tether. Very low twist might make a difference. A third parameter is the braid tightness. That would tend to affect the amount of hysteresis in slip-stick effects, with tighter braids having more hysteresis (which might be good). A fourth parameter is the selecting either Spectra vs Dyneema, and what strand denier to use. The different materials and deniers have different fiber diameters, and that might make a difference. A fifth parameter is the possibility of adding either a lubricant (to ease slippage between fibers) or a small amount of some

matrix (to try to PREVENT slippage). It's hard to get good lubricant properties over a wide temperature range, and keep the lubricant on tethers exposed to hard vacuum. And polyethylene tends to have low friction to start with, but it may be worth testing tethers with Braycote (a very low vapor-pressure lubricant often used in space). A matrix would make the whole construction somewhat springy in bending. The last option is to make the tether out of a monolithic thin flat strip of oriented polyethylene film. It might be like a thin strip from a material similar to an ordinary grocery bag. It would be stiff due to the monolithic nature, but it could be thin enough to be fairly flexible. During Phase II, we will investigate these issues further, and recommend the optimum tether material and structure for PTFF.

III. PTFF TECHNOLOGICAL READINESS ASSESSMENT

The present Phase I study estimated the NASA TRL readiness of the proposed concept based on the open non-classified literature and information. The summary of the assessment is provided in Table 2.

Table 2. The estimated NASA TRL for the key components of the proposed PTFF.

Necessary Technology	TRL Assessment	Note
Intracavity Photon Thrusters	TRL 3	Analytical and experimental critical function and/or characteristic proof-of-concept
Interferometric Ranging System	TRL 5	Component and/or breadboard validation in relevant environment
Tether System	TRL 6	System/subsystem model or prototype demonstration in a relevant environment (ground or space)
System Integration and Control	TRL 2	Technology concept and/or application formulated

We have thoroughly studied the required technologies for implementing intracavity photon thrusters. We have shown that the concept has been demonstrated in the laboratory experiments and all the necessary components are readily available off-the-shelf. The proof-of-concept has been demonstrated in such experiments. This puts the TRL of the intracavity photon thrusters 3. During Phase II, the further engineering studies will be performed to optimize the characteristics of the intracavity photon thrusters for PTFF applications.

The nanometer accuracy interferomeric ranging system has been demonstrated in breadboard setup in space-like environment. (Jeganathan, 2000, and Bender, 2003) Therefore, this sets the TRL of the interferometric ranging system 5.

The tether subsystem has been demonstrated numerously in space, thus this sets the TRL of the tether system 6.

The overall system integration and control of PTFF has been formulated, thus this sets the TRL of the overall system integration and control 2. We are confident that this TRL can advance fast, once the development program is sufficiently funded, because all subsystems have higher TRL.

In terms of Research & Development Degree of Difficulty Scale the proposed concept was classified under $R\&D^3$: II - III (moderate -high): Requires to optimize photon thrust design based on the current laboratory system and system integration, and to develop control system.

IV. MISSION SPECIFIC APPLICATIONS

Station keeping maintaining the relative inter-spacecraft distance for the next generation NASA missions to nm requires the knowledge on details of potential perturbative forces in specific orbits. Two types of station keeping are important: 1) relative station keeping and 2) absolute station keeping. The relative station keeping is for maintaining the inter spacecraft distance to nm accuracy, which is handled by the proposed PTFF system. In most of missions, the relative station keeping is much more important than the absolute station keeping. However, this does not exclude the need of the absolute station keeping, because it is needed for various major maneuvers, such as orbit correction and slewing. For example, the frequency of the operational requirement for the conventional orbit correcting thrusters depends on the mission nature.

For various reasons presented above, it is highly desirable to be able to perform the absolute station keeping with the PTFF system without adding conventional thrusters. According to our preliminary estimate, this is indeed highly feasible. For example, let us consider 2-satellite 1-km-baseline formation flying system that would need 3 photon thruster systems, and each photon thruster has a 100 W pump diode laser which require 200 W input power. Let us assume that the weight of each satellite is 100 kg, and the pump diode lasers are directly used for without the intracavity arrangement, for slewing. The thrust force on each satellite due to the total 300 W photon emission of all 3 pump diodes is about 0.5 μN, and the corresponding acceleration a is 10^{-8} m/s^2. If we assume that the structure accelerate to reach the halfway point and then decelerate to the final point, the time requires for slewing by is given by

$$t = 2\sqrt{\frac{2L}{a}} \tag{15}$$

where L is the distance that each satellite to travel to have slewing. For 1 degree slewing, L= 17.5 m, thus t = 1.18 x 10^5 sec, or 1.37 days. For 10 degree slewing, t = 4.33 days. Therefore, even with conservative power setting the major slewing can be achieved in a reasonable time without the need of other conventional thrusters.

Although, the slewing is slow, the alignment accuracy with the PTFF is unprecedented. The diode laser pump beam can be turn and off typically within 1 sec, or if more precision is required, a mechanical chopper can be used to achieve 1 sec operation time. In this case, the slewing angle accuracy would be 2x10^{-11} rad = 4 micro-arcsec. The laser beam can be chopped to have 10 msec operation, the angle accuracy would be 0.4 nano-arcsec. Therefore, PTFF is able to provide the unprecedented target alignment accuracy. The scanning accuracy is limited by the 1 nm baseline accuracy, and it is in the order of 0.1 micro-arcsec for 1 km baseline system

The system requirement for orbit correction depends on the specificity of missions. During Phase I, we only consider the relative station keeping requirement of formation flying in various mission specific applications. The method of absolute station keeping with the PTFF system will be studied more in detail in Phase II.

In this section, we show that the various perturbation forces on the relative position of the formation can indeed be countered by PTFF system efficiently.

A. Low Earth Orbit (LEO) Applications

A.1. Atmospheric Drag Effect

In LEO, atmospheric drag is the dominant orbital perturbation, which removes energy from the satellite and leads to a decrease in orbital altitude. The atmosphere drag, F_D, on a spacecraft in low earth orbit is given by the formula (LaPointe, 2001):

$$F_D = \frac{m\rho V^2}{2B} \tag{16}$$

where m is the spacecraft mass, ρ is the atmospheric mass density at a given orbital radius, V is the orbital velocity, and B is the ballistic coefficient, given by:

$$B = \frac{m}{C_D A} \tag{17}$$

where A is the spacecraft cross sectional area in the direction of motion, and C_D is an empirical drag coefficient, with value typically ranging from 2 to 4.

The orbital velocity, V, is approximately given by:

$$V = \sqrt{\frac{GM}{R}}, \tag{4}$$

where G is the universal gravitational constant, 6.6726×10^{-11} N-m^2/kg^2, M is the mass of the earth, 5.976×10^{24}kg, and R is the orbital radius with respect to the earth's center. By combining Eqns. 2 – 4, we obtain:

$$F_D = \frac{GMC_D \rho A}{2R} \tag{18}$$

Fig. 14 plots typical drag forces encountered in LEO for a range of spacecraft cross sections, at altitudes ranging from 200 km to 1000 km, which is an excerpt from the reference (LaPointe, 2001). The microsat with a mass of 100 kg and a cross sectional area of 1 m^2, and total available power of 100 W, the final laser energy can be in the order of 20 W assuming electrical power to laser photon power conversion efficiency of 20 %. Assuming the intracavity multiplication factor of 20,000 the maximum thrust produced by the photon thruster is 2.68 mN. Thus, the photon thruster can counter the inter spacecraft force up to 2.68 mN. Assuming, each spacecraft in formation may have the differential drag up to the maximum drag, the present system can station keep in relative motion down to about 400 km in LEO. Although the present system can keep the absolute distance between the spacecraft with nm accuracy, it does not counter the absolute drag applied to the whole formation flying assembly. Such an overall drag may be occasionally corrected by conventional microthrusters.

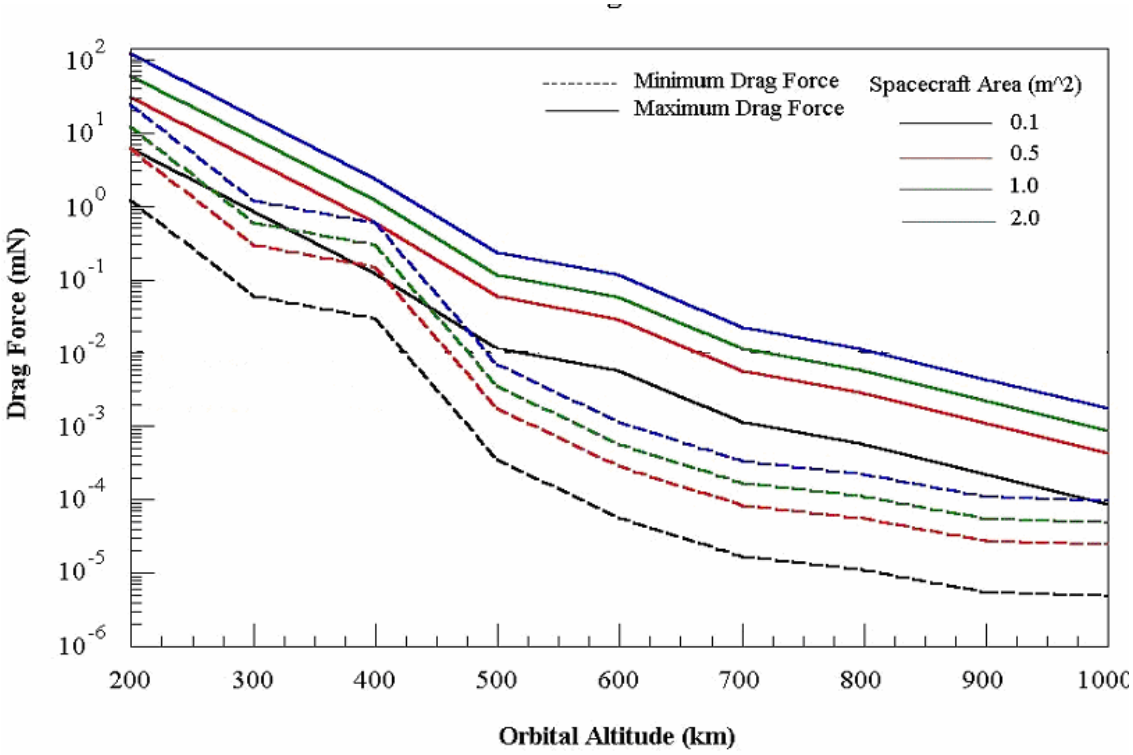

Figure 14. Atmospheric drag forces encountered in LEO for a range of spacecraft cross sections, at altitudes ranging from 200 km to 1000 km. Quoted from LaPointe, 2001.

A.2. Gravity Gradient Effect

More important than the atmospheric drag effect in LEO tethered formation flying structures is the gravity gradient effect. Because the satellites in tethered formation orbits at the same angular velocity, thus with same centrifugal force, the gravitational force does not cancel out resulting in the gravity gradient effect. If we consider 1-D two satellite configuration vertically aligned to the earth center of the mass, the gravity gradient effect between the satellites, F_{GG} is given by

$$F_{GG} = 3L_T m\omega_0^2 \tag{19}$$

where L_T is the tether length, m is the mass of the satellite and ω0, the angular velocity of the center of the mass of the formation is given by

$$\omega_0 = \sqrt{\frac{GM}{r_0^3}} \tag{20}$$

where G is the universal gravitational constant (6.673 x 10^{-11} Nm^2/kg^2), M is the mass of the Earth (5.979 x 10^{24} kg), r_0 is the radius of the system's center of gravity from the center of the Earth (m) (Cosmo,1997). From this equation, one can obtain that for LEO the equivalent acceleration per km of the tether length, a_{GG}, is ~ 3.5 x 10^{-4} g/km, and for GEO, ~1.6 x 10^{-6} g/km.

For 100 km satellites LEO formation with 1 km tether the maximum gravity gradient can be ~35 mN, which is one order of magnitude larger than the atmospheric drag at the altitude of 400 km. Therefore, in PTFF LEO applications, the dominant major perturbation is the gravity gradient.

In the pentagonal pyramidal formation flying structure with a 1 km baseline distance, the maximum perturbation experienced in a photon-tether subsystem is 35/5 = 7 mN. The compensation of this force would require about 50 W photon thruster systems with the intracavity multiplication factor of 20,000. This power requirement is still within the power budget of 100 kg microsatellites, therefore, the PTFF can be used in LEO applications, if the 20,000 intracavity multiplication is feasible. If the maximum achievable intracavity multiplication factor is less, then the required power for the photon thruster is larger.

B. Geosynchronous Earth Orbit (GEO) Applications

Although atmospheric drag forces are considerably decreased in GEO, other orbital perturbations become more significant. These additional perturbations include effects

on the satellite orbits due to the oblateness of the earth, earth triaxiality, sun-moon perturbations, and, at sufficiently high orbits, radiation pressure from the sun.

However, the effect of solar pressure impinging on a satellite can induce the differential force depending on the shape and orientation of the spacecraft. The solar perturbing force, F_S, on a satellite of mass M and surface area A is given by: (Lovell, 1973)

$$F_S = S(1+\sigma)A \tag{21}$$

where S is the solar constant at 1-AU, 4.5×10^{-6} kg/(m-s^2), and σ is the average reflectivity of the satellite. Assuming a microsatellite mass of 100-kg, a cross-sectional area of 1-m^2, and an average reflectivity of 0.5 yields an in-pane maximum relative perturbation due to solar radiation pressure of approximately 6.8×10^{-6} N. This can be easily countered the current system, which can provide the thrust up to 2.68 mN.

The maximum gravity gradient effect on PTFF with a 1 km baseline distance in GEO is about 1.6×10^{-4} N, which is more than one order of magnitude larger than other perturbation effects. Therefore, even at GEO, the dominant perturbation force is the gravity gradient force. However, this can be countered readily with a 20 W photon thruster system.

C. Lagrangian and Other Orbit Applications

For the future NASA astronomical observations, significant advantages in satellite station-keeping may be achieved by positioning the formation-flying array in a stable Lagrangian orbit or into a heliocentric earth-trailing orbit. A number of formation flying concepts have been developed to take advantage of the stability provided by Lagrangian orbits and heliocentric fall-away trajectories. For a planet moving around the Sun, there are five Lagrangian points in space at which spacecraft remains in a stable orbit with respect to the planet. In this case, because the spacecraft does not orbit the planet, perturbation forces from atmospheric drag or planet triaxiality do not affect a formation flying, and only solar radiation pressure should be countered. As shown before, the relative perturbation due to solar radiation pressure can be readily countered by the present system. Therefore, the proposed ultraprecision formation flying is also suitable for Lagrangian and other orbit applications.

V. EXEMPLARY MISSION STUDIES

In addition to redefining and simplifying the existing NASA mission concepts, such as SPECS and MAXIM, the present concept enables other emerging revolutionary NASA mission concepts, such as X-Ray Fourier Transform Spectrometer proposed by Dr. Schnopper and New World Imager Freeway Mission proposed by Prof. Cash, which searches for advanced civilization in exo-planets. As the present concept is more publicized, many other exciting concepts are expected to follow. One of such possible missions is the construction of ultralarge space telescope with diameters up to several km for observing and monitoring space and earth-bound activities. In this Phase I report we highlight several new potential NASA missions, and more detail studies on engineering specificities of the existing NASA mission concepts and the following new concepts will be performed during Phase II.

A. Ultralarge Adaptive Membrane Telescopes

Many of NASA's future missions require to build much larger space telescopes than those available today, such as the *Hubble Space Telescope* (HCT) with its 2.4 m primary mirror. Although HCT has provided significant information about outer space during the last 10 years, much higher resolution is required to unlock the secrets of the universe. Because the diffraction-limited angular resolution of a telescope is proportional to the aperture diameter, larger and larger size space telescopes are desirable for both the astronomical and Earth-observation communities for the future missions.

Currently, for a monolithic space telescope, the size of launch vehicles is the major limiting factor, thus mass-optimal telescope construction is crucial in increasing the telescope size. For a reflector telescope two major types of mass-optimal design are currently researched in reducing the size and weight: 1) membrane telescopes and 2) sparse aperture telescopes. The membrane space telescope would consist of a reflective layer just thick enough to reflect the science wavelength. Such a thin mirror will have little bending stiffness and will behave as a membrane over large diameters.

According to the physics of large telescope design for an on-axis, filled-aperture reflector, the standard wavefront error RMS requirement is 1/10 the wavelength. For the visible wavelength space observation, thus, the RMS position requirement across the whole mirror is hundreds of nanometers. The structural support of the membrane plays different interacting roles. First the rim must be positioned to tolerances similar to the mirror requirements over the entire circumference. Next the rim support must provide enough stiffness to be the reaction structure for the application of membrane tension. Lastly, the rim support connects the membrane to the rest of the telescope structure. Therefore the membrane mirror rim support must provide a highly accurate

and stable mirror boundary condition while receiving disturbance inputs from other locations in the spacecraft (de Blonk, 1999).

PTFF may be a key technology enabling an Adaptive Membrane usage for the future ultralarge telescopes with the diameters of kms. Fig. 15 shows an artist's concept of such an ultralarge Adaptive Membrane telescope. The baseline polygon formation structure (a pentagon in this example) of PTFF can create tension in the membrane surface and actively change the curvature for a wide range of optical resolutions in conjunction with the baseline structure rotation along the axis electric dipole interaction in the membrane as in Stretched Membrane with Electrostatic Curvature (SMEC) Mirrors. In SMEC, the curvature of the membrane mirror can be adjusted by the electrostatic potential applied across the membrane. (Errico, 2002) A PTFF secondary mirror or membrane can also be flown as part of the system. According to the research data (Stamper, 2001), the useful area of the membrane with 5 point attachment is over 80 % of the total membrane area, thus the need of the continuous attachment is not necessary.

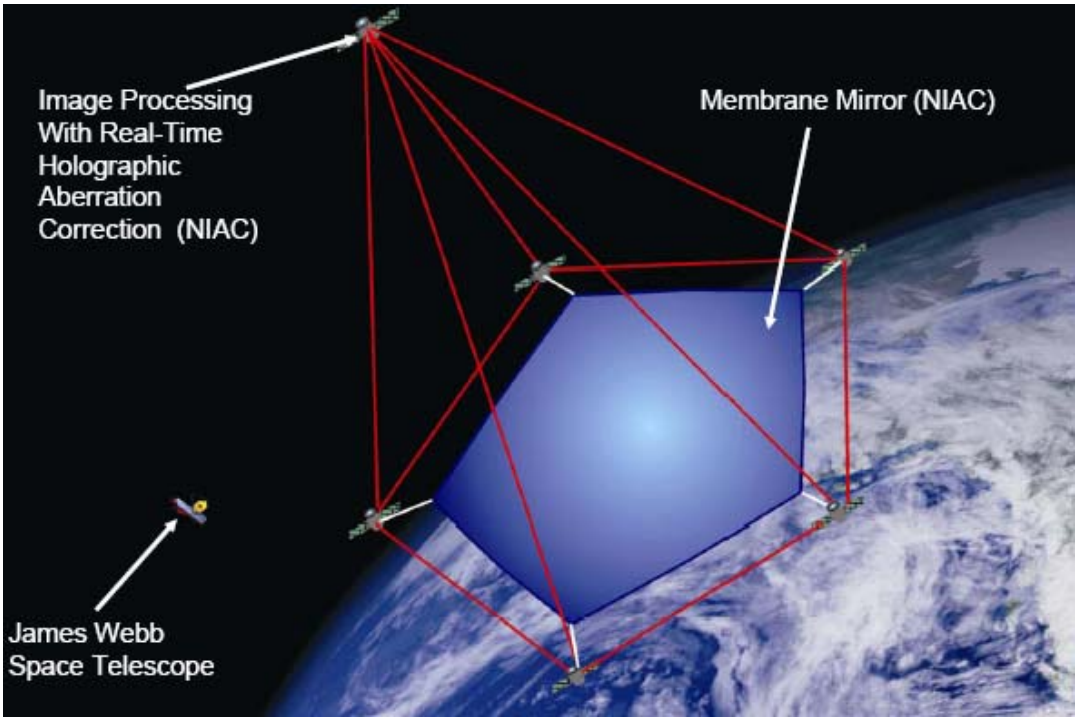

Figure 15. An artist's concept of such an ultralarge Adaptive Membrane telescope formed by pentagonal pyramidal PTFF. The 5-point attachment membrane has over 80 % optically useful area according to the recent research result. (Stamper, 2001) The small structure shown left of the PTFF telescope is a conceptual design of NASA James Webb Space Telescope (JWST) for relative size comparison.

One of the major concerns about using the membrane for the telescope is the flatness achievable with the currently available manufacturing technology. With the currently available manufacturing technology, Polymeric materials with extremely low CTE such as polybenzoxazole (PBO) have been predicted to have an onorbit surface in accuracy of only 0.35 mm RMS, which is nearly 3 orders of magnitude larger than the required RMS accuracy for visible wavelength space imaging. Once the membrane telescope area is revitalized considerably in the near future, the RMS surface accuracy is expected to become rapidly much smaller than the currently available one.

Even though the manufacturing surface RMS accuracy is achieved in the desired level of several hundreds of nanometers, other environmental perturbation effects, such as membrane vibration and thermal expansion/contraction will decrease the RMS surface accuracy during the telescope operation. For example, membrane reflectors on the order of 10 m diameter made from Kapton-E with ten times larger coefficient of thermal expansion (CTE) than PBO, have been shown to have ~1 mm rms surface inaccuracy. The surface RMS fluctuation of PBO is expected to be smaller than that of CTE. Exact RMS surface accuracy fluctuation will depend on the mission characteristics and membrane material. Holographic techniques have been improved considerably to the point that surface inaccuracies on the order of 1 mm rms or less are perfectly correctable to the diffraction limit. Hence, a spherical or parabolic mirror made of a thin film of PBO in conjunction with the proper holographic correction can enable a 10m or larger space-based aperture operating in the diffraction limit. (Palisoc, 2000)

Therefore, PTFF is a key technology in the creation of an Adaptive Membrane for imaging, a system which can change the design of future telescope systems. Figure 14 shows a onceptual drawing of what this system may look like. A ring of PTFF spacecraft can create tension in the membrane surface and actively change the curvature for a wide range of optical resolutions. An PTFF secondary mirror or membrane can also be flown as part of the system. PTFF is a critical technology because it has the ability to uniquely change the shape, size, and tension of the membrane surface and possibly surface components using electric dipole interaction.

B. New-World-Imager and Freeway Mission

The ultralarge PTFF membrane telescope can be used for many future NASA missions for obtaining the pictures of planets around stars. For example, one of the most ambitious future proposed NASA missions is the “Freeway Mission,” proposed by Prof. Cash (Cash, 2005) that will be able to study the exo-planets in same way that LandSat and other Earth-observing systems study the surface of the Earth. The exo-planets are the earth-like planets formed in other star systems.

Science fiction authors have always assumed we would have to visit distant planets to obtain images like Fig. 16, but they can, in principle, be captured from light years away.

Such a telescope will of necessity be large, to collect enough light to resolve and analyze small details on distant planets. To capture the needed signal takes square kilometers of collecting area, that has considered to be a practical impossibility for the foreseeable future to date. (Cash, 2005). The above mentioned PTFF ultralarge km diameter membrane telescope should enable such a mission so that the mission cost would be within the envelope of what NASA can afford.

Figure 16. From the movie Contact. Dr. Arroway gets a brief glimpse of this alien landscape. Such images are possible from Earth, although, at the moment, very expensive. However, PTFF is capable of providing the crucial step towards obtaining such an image. Excerpt from Cash, 2005.

C. 1-D Formation Flying Structure for Fourier Transform X-Ray (FTXR) Interferometer

Fourier Transform Spectrometry has revolutionized the optical spectroscopy in the last century. In particular, Fourier Transform Infrared (FTIR) Spectrometry has been extensively used for numerous scientific and engineering applications. The innovative concept by Dr. Schnopper (Schnopper, 2006) to apply a Fourier transform X-ray interferometer to the spectral diagnosis of hot, X-ray emitting, cosmic plasmas is a revolutionary idea. This concept fits nicely into the goals of the Beyond Einstein long range mission planning program. The feasibility of this concept relies on exploiting the results from a suite of state-of-the-art technologies developed in four disparate areas: nanopositioners with picometer precision; flat, ultra smooth (~0.05 nm rms) silicon crystals; ultra thin (~1 μm) polymide membranes; and ultra thin (~0.8 nm) bi-layer deposition technology. X-ray Fourier Transform Spectrometer concept for high resolution X-ray spectroscopy "leap-frogs" the solid state, cryogenically cooled, microcalorimeter spectrometers now under study for NASA's CONSTELLATION-X and ESA's XEUS, advanced X-ray spectroscopy missions. We can achieve a spectral resolution of one part in 10^4 (and set a goal of 10^5) from highly excited ions of C through

Fe (with considerably higher energy resolution than a microcalorimeter). Instead of merely seeking to identify constituents and their abundances in the hot plasma we will be able to "resolve" their line shapes. Some of the science, thereby enabled, is based on structural dynamics (velocity distributions) rather than on diagnostics. Fourier Transform X-Ray Spectrometer will map the emission and absorption structure from ions heavier than oxygen near black holes, in stars, and in the intergalactic medium. We can make these high resolution observations on heavily absorbed objects, where the resolution of wavelength dispersive spectrometers at high energies is low. We have chosen to study the wavelength range (~0.1 to ~4 nm) that encompasses the principal H- and He-like emission lines from abundant species from C through Fe. We require a separation of >100 m between the ~1 m diameter X-ray telescope and the interferometer. This requirement can be met by the development of an ultra-precision boom or two satellites flying in tightly controlled formation.

The present Photon Tether Formation Flight (PTFF) method enables the most stringent formation flying required by the above-mentioned Fourier Transform X-Ray Spectrometer. An example of conceptual design of the overall 1-D PTFF system for this mission is shown in Fig. 17. The sub-nm precision station keeping between two spacecraft is performed by three photon thrusters, three tether systems, and three interferometric ranging systems, which allows ultrahigh precision attitude and directional control of spacecraft as well. The integration concept of PTFF and FTXR is illustrated in Fig. 18. The PTFF enables the FTXR's operation in space by providing sub-nanometer accuracy one-dimensional formation flying structure with a baseline of ~10 km. The more in-depth engineering details will be studied in Phase II.

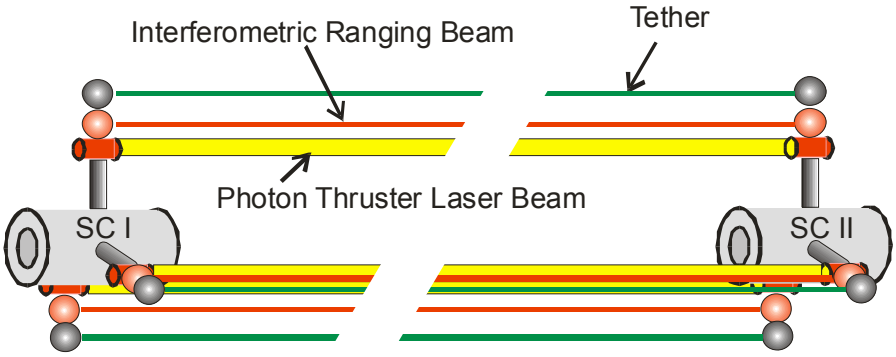

Figure 17. An artist's concept of 1-D PTFF structured by two spacecrafts and three photon thrusters, three tether systems, and three interferometric ranging systems.

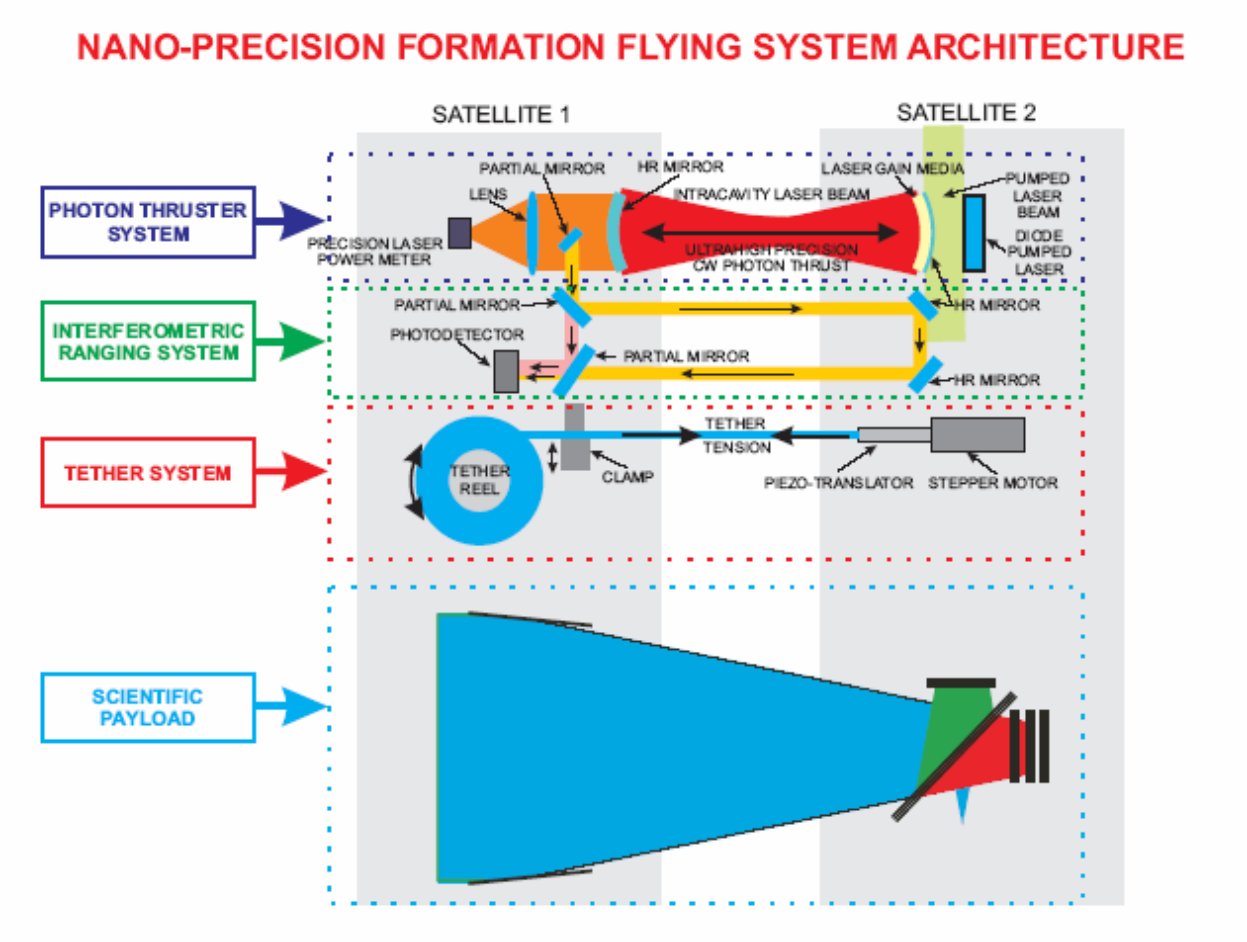

Figure 18. The conceptual design of Fourier Transform X-Ray (FTXR) Interferometer combined with Photon Tether Formation Flight (PTFF) method. The PTFF enables the FTXR's operation in space by providing sub-nanometer accuracy one-dimensional formation flying structure with a baseline of ~10 km. The figure only shows one photon thruster, interferometric ranging system, and tether system, however, in the actual application, the three such combined systems are required as shown in Fig. 17.

One of the technological concerns of 1-D structure is the bending modes or lateral shift of the structure. Most of the envisioned mission concepts are insensitive to this bending or lateral shifting. For example, the primary requirement for the FTXR is that the axis of the telescope remains aimed at the interferometer with a precision of about 0.1 arcsec (at 10 km) and 1 arcsec (at 1 km) (Schnopper, 2006). These tight specs will insure that the beam will fall on the interferometer.

Let us assume that two spacecraft are separated by L, and there is a relative lateral shifting of δy as shown in Fig. 19.

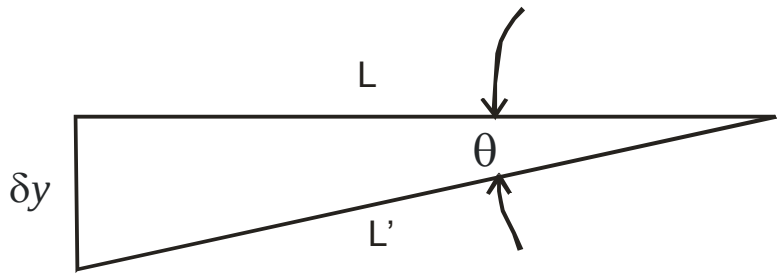

Figure 19. The relationship between the increase in the baseline distance and the lateral shifting of the 1-D formation structure.

In this case the angle θ is given by

$$\theta \sim \frac{\delta y}{L}. \tag{22}$$

The increase in the baseline distance, δL, is given by

$$\delta L \sim L' - L = \frac{L}{\cos\theta} - L. \tag{23}$$

At small angle θ, 1/cosθ is given by

$$\frac{1}{\cos\theta} \sim 1 + \frac{\theta^2}{2}. \tag{24}$$

Therefore, δL, is given by

$$\delta L \sim \frac{\theta^2}{2} L. \tag{25}$$

For a 1 km system, $L=10^3$ m, θ =1 arcsec = 4.8×10^{-6} rad, thus, δL ~ 1.2×10^{-8} m= 12 nm. Therefore, if the baseline distance is maintained better than 1 nm, the overall shifting angle can be controlled better than 0.1 arcsec for a 1 km baseline system.

For a 10 km system, $L=10^4$m, θ =0.1 arcsec = 4.8×10^{-7} rad, thus, δL~1.2×10^{-9} m= 1.2 nm. Therefore, the lateral shifting tolerance can be controlled by the present PTFF system.

VI. DESIGN OF PHOTON THRUSTER AND NANO-PRECISION THRUSTER TEST STAND FOR PHASE II

The proof-of-the-principle of the photon thruster has been demonstrated in numerous laboratory experiments by other researchers, who especially work on the cavity ring down spectroscopy. In the cavity ring-down system, the laser pulses in the cavities are routinely bounced between two high reflectance mirrors as much as 10^4 – 10^5 times (Romanini, 1997). In other laser setups where the intracavity power multiplications are used for frequency doubling and mixing. In this case, the intracavity laser power multiplication factor is typically in the order of 100 (Lee, 2004). The photon thruster operation range should be similar to that of the cavity ring-down laser system, except the gain media is in the cavity as in the intracavity frequency doubling and mixing system. To maximize the intracavity gain, the absorption through the gain medium and reflective loss on the surface of the medium should be minimized.

One of the crucial parameters in engineering the photon thruster is the maximum intracavity power multiplication factor, i.e., the maximum number of bouncing of photons between the cavity mirrors. The typical present day laboratory and industrial lasers do not operate in this cavity design parameter range, rather, they are designed to generate the maximum extra-cavity laser beam power and quality. To maximize the intracavity laser power, the gain medium should be designed much different from the existing laser systems.

During Phase II, we plan to address the following issues regarding the intracavity laser system engineering design:

1. The optimum laser system
2. The optimum design of the gain medium to minimize the absorption and scattering loss through,
3. The optimum pumping system design (side pumping or end pumping),
4. The optimum design of the thermal management system of the medium
5. More detailed optical studies on the diffraction loss of the mirror,
6. More detailed optical studies on the optimum geometry of the HR mirrors.

Some aspects of these issues can be addressed theoretically with the use of existing software, such as ZEMAX, however, the laser system and gain medium related issues should be addressed experimentally. During Phase II, we plan to build a 1 W extracavity power photon thruster that consists of an intracavity YAG laser pumped by a diode laser to research the above issues. Initially, when we wrote the Phase I proposal, we contemplated to investigate the photon thruster concept with a 10 W system for Phase II, primarily to produce enough thrust to be measured the typical torsion thruster stand.

During this reporting period we have learned that this will cost most of the research budget for Phase II leaving not enough resources for other crucial studies, such as formation dynamics simulation studies. Since the importance of the realistic tether simulation is crucial, we have to reduce the budget for the photon thruster demonstration. In fact, for the optimum engineering parameter studies on the photon thrusters in Phase II, a 1 W laser system would be sufficient. Currently, at a reasonable cost, a diode pumped YAG laser with the maximum power of 1 W for the laser media composed of a YAG, and diode laser pumping arrangement available commercially.

We plan to build the photon thruster demonstration prototype system with the off-the-shelf Newport Supermirrors with a reflectance of 99.97 %. This photon thruster is predicted to provide the thrust of 22 μN. To measure such thrust confidently requires a thruster stand setup able to measure with tens of nN accuracy reliably. During Phase I, we have designed such a thrust stand system that can be readily coupled with the photon thruster for Phase II. The schematic diagram of the proposed propulsion system is shown in Fig. 20. The thruster stand for measuring such thrust was very complicated and expensive to build with the previous arts. However, Phipps and coworkers (Phipps, 2005) have just developed an ideal thruster stand for our proposed research. The thruster stand is relatively straightforward to build and able to provide a 25 nN accuracy with the use of laser interferometry.

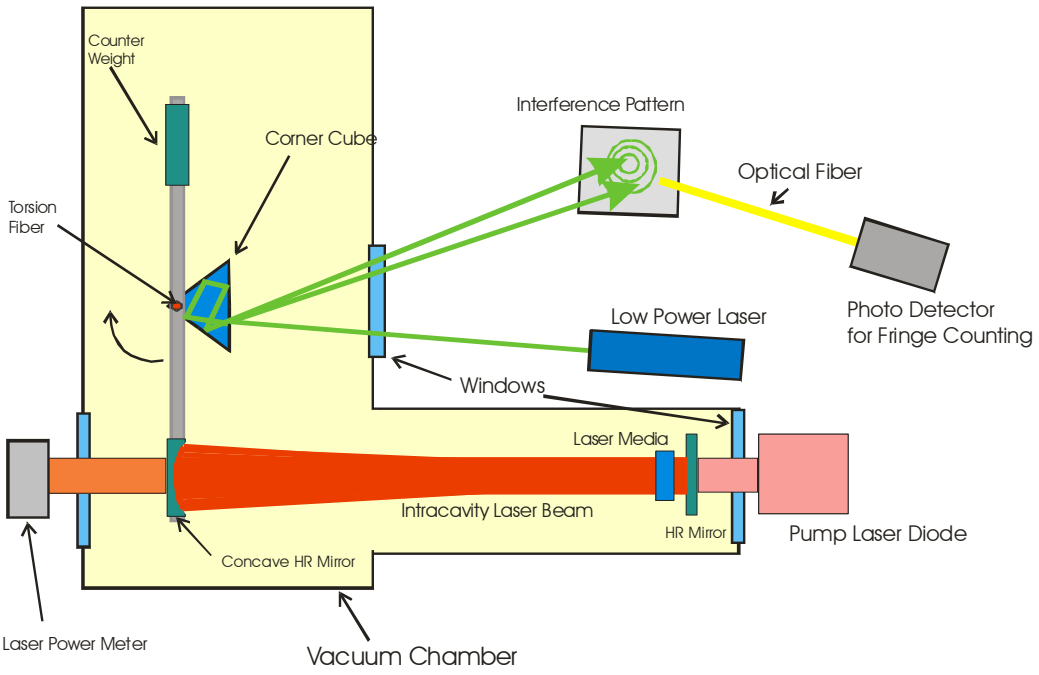

Figure 20: 1 W experimental setup for demonstration of the preprototype photon thruster capable of delivering thrust up to 134 μN in the nN thruster stand with 25 nN accuracy. The thrust is measured by a torsion fiber system coupled with laser interferometer and corner cube in vacuum.

In Phase II, the laser output will be measured with a laser power meter as a function of the pump diode laser input power and photon thrust between two mirrors will be measured with the nN thruster stand. In Phase II, we plan to start with a 50 cm long intracavity, and try to develop the technique to increase the length of the intracavity to several m. The intracavity photon thruster outside of the vacuum chamber will be enclosed in an inert gas environment to minimize the intracavity absorption. The cavity system is very sensitive to the vibration and structural noise of the system. An active mirror controlling system will be developed to compensate the building and equipment structure vibration. Such an active mirror controlling system will be highly crucial to the real implementation of the system. In the real system, the mirror system perturbation will result from the tether control system. In Phase II, the mirror control system will be refined such that it can handle the vibration and noise from the tether control system upon integration of the whole system.

Fig. 21 shows the vacuum thrust stand setup. The test stand setup will be similar to that developed by Phipps et al. (Phipps, 2005). The entire setup will be mounted in a vacuum test chamber. The details of the thruster test stand are shown schematically in Fig. 20.

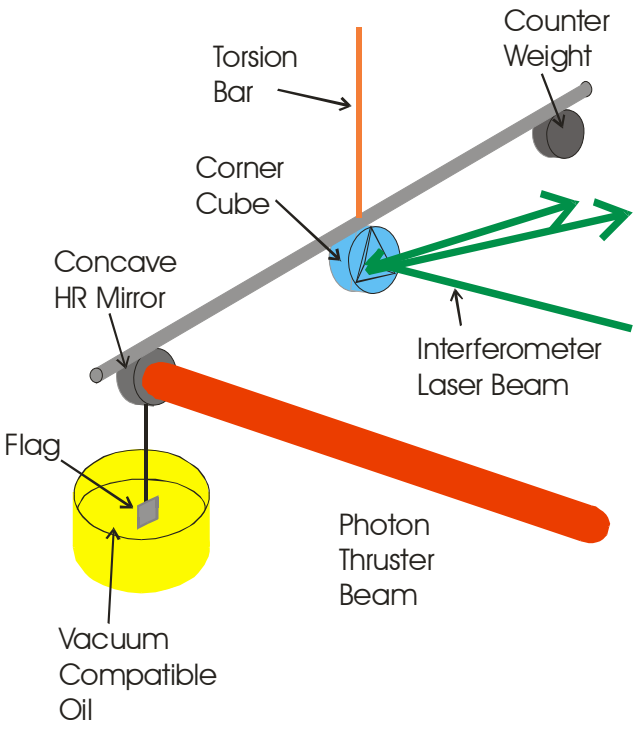

Figure 20. Detailed schematic diagram of the thruster stand with 25 nN accuracy.

The test stand will use a torsion bar, a critical damping attachment with a flag immersed in diffusion pump oil, and an optical corner cube for interferometer. The measured thrust F is given by

$$F = \frac{k\theta}{R} \tag{26}$$

where *K* is torsional spring constant given by

$$k = \frac{\pi d^4 G}{32L} \tag{27}$$

where *G* is torsion modulus, *L* is effective length, *J* is the polar moment, and *d* is diameter of the torsion fiber.

With the fused silica torsion fiber of 78 μm diameter, k = 194 pN-m/μrad and R = 0.155m, so that k/R = 1.25 nN/μrad. To have the thrust stand to have 25 nN precision, the rotation sensor must resolve 20μrad bar rotation. An interferometer based on a solid glass retroreflecting "corner cube" (described below) is the key to resolving rotation of the bar. Critical damping is provided by a flag immersed in diffusion pump oil. The retroreflector, a solid glass corner cube, with a 2.54cm diameter aperture will be used for reflecting the laser beam. The two reflected beams from the front surface and from internal reflection of the corner cube will be combined on a surface creating interferometric fringes. A 5 mW, 532-nm near-diffraction-limited CW beam expanded to 15mm collimated diameter using a beam expansion telescope. As rotation occurs, these fringes move radially outward or inward, depending on the direction of rotation of the bar. Counting the passage of the fringes, which can be done visually or using the figure 3 setup, gives rotation. Phipps et al. (Phipps, 2005) reported that this setup was able to resolve 20 μrad bar rotation resulting in the thruster measurement accuracy of 25 nN, sufficient enough for the Phase II demonstration.

VII. ROADMAP

A. Predictions and Limitations on PTFF

In science, whenever an instrument has increased its accuracy/capability by orders of magnitude, it has opened up numerous applications, and often new scientific fields. Some of the major revolutionary examples are listed below in the order of dimension:

1. Subatomic Dimension
High Energy Accelerators: By increasing the acceleration energy, thus decreasing probing dimension in subatomic particles by orders of magnitude compared with previous accelerators.

2. Atomic Dimension
Scanning Tunneling Microscopy/Atomic Force Microscopy: By increasing the scanning resolution by orders of magnitude with minimal disturbing of the observed system compared with other microscopy systems.

3. Molecular to Day-life Dimension
Laser: By increasing the spectral purity and the focusing capability by orders of magnitude compared with incoherent light sources.

4. Astronomical Dimension
In the astronomical dimension, one of the most important goals is to increase the imaging resolution of the target, which is inversely proportional to the diameter of the observation apparatus aperture. The potential revolutionary breakthrough in the astronomical dimension has been recognized by NASA to be the precision formation flight that enables ultralarge aperture platforms that are able to increase the aperture size by many orders or magnitude, surpassing the one constructible on earth at the budget within reach. Size limitations on launch vehicle fairings leave formation flying as the only option to assimilate coherent large apertures or large sample collection areas in space (Leitner, 2004). In particular, the formation flight technology with the ultrahigh baseline accuracy at 100 m to several km baseline lengths is the key technology for enabling such ultralarge aperture platforms. Thus far, a solution for maintaining a precise spacecraft configuration in space has proven illusive.

With the currently available microthruster technologies, the spacecraft formation structure with the baseline accuracy in the spacecraft formation structure of 1 cm is feasible. PTFF, if fully demonstrated, is predicted to increase the currently available accuracy by seven orders of magnitude. It is too early to compare the potential of PTFF in opening new concepts and possibly new scientific fields with the above mentioned major revolutionary breakthroughs in 20th Century; however, PTFF is predicted to result

in new concepts and scientific fields by quantum leaping in the baseline accuracy in the spacecraft formation structure in the astronomical dimension.

By investigating the limitation of the technology, it is possible to predict the overall potential of the proposed concept. In this section we review some of the limitations on the eventual performance of PTFF in enabling new science and engineering concepts.

A.1. Limitation on the Baseline Size

The limitation on the PTFF baseline size is determined by the HR mirror diameter in the photon thruster. With the currently available technologies, the HR mirror diameter in the order of 1 m is possible. However, considering each spacecraft should carry possible 3 such HR mirrors, the weight of the mirrors probably sets the limitation, rather than their size. For microsatellites, it is possible to carry three 20 cm diameter HR mirrors, resulting in a baseline size limitation of 10 km. For a larger spacecraft missions, if the weight of HR mirrors is not of major concern, the current mirror (1 m diameter) technology sets, the baseline size limitation to be ~200 km. For the missions requiring much larger baseline dimensions, such as LISA, PTFF is unsuitable.

A.2. Limitation on the Baseline Accuracy

The limitation on the baseline accuracy of PTFF is determined by the accuracy of the tether control system and/or the laser interferometric ranging system. The accuracy of off-the-shelf piezo-translators is in the order of 0.1 nm. The accuracy of the state-of-the-art interferometric ranging system is in the order of 1 nm. Therefore, the current limitation of PTFF baseline accuracy results from the limitation of the interferometric ranging system, and it is in the order of 1 nm.

A.3. Limitation on the PTFF Lifetime

There are many factors limit the lifetime of PTFF. Two of the most important factors are the lifetimes of the pump diode laser of the photon thruster and the tether. Currently, the lifetime of the diode pumped solid state lasers at full operation power is limited by that of pump diodes to about 10,000 hours (1 year) for continuous operation. With the reduced power operation or discontinuous operation the lifetime of the pump diodes is expected to be longer. In any case, the overall lifetime of the system can be further extended by simply replacing the pump diodes with new ones. With a ten unit carousel, for example, the lifetime of the system is extended to tens of years. Moreover, with the rapidly developing diode laser technology, the lifetime is expected to increase significantly over the next decade.

The lifetime of the tether in the space environment is another critical limiting factor on the lifetime of PTFF. In general, the lifetime in LEO can be considered to be the lower bound for the lifetime in other orbits, thus, in this report the breakdown of tethers in LEO operation is analyzed. The lifetime analysis of the tether based on the effect of meteoroid impact predicts that a 1 km tether with a diameter of 1 mm has a lifetime 2.2 years, and a 4 mm tether 80 years. The tether lifetime in other orbits is expected to be much longer.

In sum, with a reasonably thick tether (in the order of mms), the limitation factor on the PTFF lifetime is mainly that of pump diodes. This can be readily increased to tens of years with the use of a carousel design.

A.4. Limitation on the Number of Spacecraft

Theoretically or physically, there is no limitation on the number of spacecraft with PTFF. For example, a 60 spacecraft structure with C_{60} fullerene structure (and other large icosahedral structures) can be envisioned with PTFF. The limitation on the number of spacecraft, currently, results from the economical affordability.

A.5. Limitation on the Orbit

PTFF relies on very subtle thrusts in the order of mN at the maximum with the total spacecraft power budget of 100 W. This sets the limitation on the nature of orbits in which PTFF can be used. One of the main limiting factors is the gravity gradient and atmospheric drag, thus, higher orbits, such as GEO and Lagrangian Orbits are preferred. If the mission requires LEO, PTFF may require higher total spacecraft power budgets or the strategic coupling of PTFF with spinning the formation.

B. Required Technologies

Most of the technologies needed for implementing PTFF already exist and need only be adapted. However, some technologies are more challenging than others. In this section we list those technologies and discuss what needs to be done below.

B.1. Photon Thrusters

One of the most important technical issues related with photon thrusters is the engineering of the intracavity system, in particular the gain medium system. The required technology for this case is the optimum laser cavity design to obtain high multiplication factors in the range of 1,000 to 10,000, and eventually over 10,000. On the other hand, if the on-board power capacity of the spacecraft is more than 1W/kg,

(with the use of nuclear power, such as RTGs, the power capacity can be much higher), the multiplication factor can be much more relaxed. In this case, the required multiplication factor is in the range of 100 – 1,000.

B.2. Nano-Meter Accuracy Interferometric Ranging System

The laboratory system for nano-meter accuracy interferometric ranging system was demonstrated in a space-like vacuum chamber. The key technical challenge is in the integration of the photon thruster laser with the design of the interferometric ranging system. In particular, the laser beam off the photon thruster should have enough stability.

B.3. Tether System

The tether system technology is more mature than other require technologies mentioned above. The required technologies for the tether system are for pre-tensioning to cure the tether, and the tether vibration controlling. Eventually, tethers specifically designed for PTFF can be engineered.

B.4. Overall Dynamics Control System

The environmental perturbation from any direction will be distributed into the 1-D force structure between paired spacecraft. 1-D structure analysis will be similar to 1-D molecular vibrational analysis. For the 1-D system the lateral shifting or bending is a major concern. However, we have shown here that the tolerance requirement to keep the x-ray beam into the detector is much more relaxed, and 1 nm baseline (axial) distance accuracy control can easily satisfy the lateral tolerance requirement for the baseline length up to 10 km. The dynamics of this issue, however, need computer simulation study. The 3-D dynamic simulation will require much more sophistication in simulation.

B.5. Launch and Deployment

The system launch and initial deployment have to be investigated thoroughly. Eventually, computer simulation would be ideal for this engineering issue. Launching of the PTFF structure can be done in a single delivery or multiple deliveries. For multiple deliveries case, the system should be assembled first before deployment. We have shown that the photon thrusters can be used for providing the expulsion force required for deployment. However, unrolling the tethers with minimal perturbation is an engineering issue, and needs further studies.

B.6. Target alignment, Scanning and Retargeting Issues

The method of scanning should be developed. For small angle scanning relative changing of the baseline distances can create the scanning. The retargeting requires major alignment angle of the formation, and requires additional thrust to the interspacecraft thrust. It was shown preliminary in this report that the major retargeting can be performed in a reasonable time scales (1 degree in a day) with the use of the pump diode laser beams directly. Although, the slewing is slow, the alignment accuracy with the PTFF is unprecedented with the accuracy of 4 micro-arcsec for 1 sec alignment time. For 10 msec alignment time, the angular accuracy would be 0.4 nano-arcsec. The scanning accuracy is limited by the 1 nm baseline accuracy, and it is in the order of 0.2 micro-arcsec. These are the order of magnitude estimate, and the more accurate numbers will be provide with further mission specific studies.

C. Phase II and Beyond

Within the limitations of a Phase I investigation, we have tried to provide the theoretical proof-of-concept, and identify and quantify the problems facing the realization of Photon Tether Formation Flight (PTFF) for the next generation NASA missions. Although the exposure of PTFF to public has been limited, it is already evident that PTFF enables other new NASA mission concepts, exemplified by the X-Ray Fourier Transform Spectrometer proposed by another NIAC fellow, Dr. Schnopper. In Phase II we propose to further improve the confidence of PTFF that NASA can place PTFF in its Roadmap.

A. Detailed Mission Design

During Phase I, we have produced a strawman design and first cut estimates of the difficulties and problems to be faced in implementing PTFF in various exemplary mission concepts. These difficulties and problems vary depending on the nature of the missions. Logically, the next step is to create a detailed mission design utilizing experts in all the various disciplines of space engineering to find an optimal solution to the problem. During the initial stage of Phase II, we propose to generate a hierarchical list of the future NASA mission concepts. Based on this list, we will try to create the detailed mission designs for the top several mission concepts.

B. Development of Required Technologies

Several technologies are required to be demonstrated for the acceptance of PTFF usage in a wide range of NASA applications. They include:

1. the intracavity photon thruster,
2. the active HR mirror controlling system for the photon thruster,
3. the nano-meter accuracy interferometric ranging system.
4. the tether system with nano-meter control accuracy,
5. the dynamical control system that combines the photon thrusters and tethers
6. the tether vibrational control system

During Phase II we expect to further investigate these key technologies and decrease the technical risk associated with each of these.

C. Implementation of PTFF in Actual Missions

The scientific and engineering community, like other communities, is often reluctant to embrace a new idea and supplant older ones. During the peer review process for the publication in STAIF in Phase I, we have answered numerous stringent technical questions about PTFF, and have generated at least first acceptance of the concept in the space community. Several reviewers scrutinized the concept, and at the end, they agreed that there is no insurmountable technological blockage for PTFF so far.

The mission concepts that would first utilize PTFF are simplest ones, such as a1-D PTFF structure for X-ray Fourier Transform Spectrometry in space, and a tetrahedron PTFF structure that could be used for the modified structure of SPECS. Other relatively simple systems are large membrane telescopes formed by PTFF. In particular, the membrane telescopes with the diameter of 10 – 100 m will be within the reach in the near future, once manufacturing issues related with the membrane uniformity is resolved. We foresee that once this membrane telescope community is revitalized due to enabling PTFF, the concurrent research on this aspect will speed up, and the desired membrane quality will be within reach in the near future.

VIII. REFERENCES

Beletsky, V.V., and E.M. Levin, 1993, *Dynamics of Space Tether Systems*, Advances in the Astronautical Sciences, Vol. 83, Univelt Inc.

Bender, P.L., Hall, J.L., Ye, J., and Klipstein, W.M., "Satellite-Satellite Laser Links for Future Gravity Missions," *Space Sci. Rev.* **108**, 377-384 (2003).

Cash, W., "X-ray Interferometry-Ultimate Imaging," NIAC Phase II Final Report, (2002), www.niac.usra.edu, accessed July 10, 2005.

Cash, W., "New Worlds Imager," NIAC Phase I Final Report, (2005), www.niac.usra.edu, accessed December 10, 2005.

Cosmo, M.L., Lorenzini, E.C., "Tethers in Space Handbook," (1997).

De Blonk, B.j., Miller, D. W., "Narrowing the Design Space of a Large Membrane mirror," (1999) http://origins.jpl.nasa.gov/meetings/ulsoc/papers/deblonk.pdf#search='Narrowing%20the%20Design%20Space%20of%20a%20Large%20Membrane%20Mirror', accessed April 10, 2006.

Fowles, G. R., *Introduction to Modern Optics*, Holt, Rinvehart and Winston, Inc., New York, New York., 1975, pp. 278-281.

Jeganathan, M., and Dubovitsky, S., "Demonstration of nm-level Active Metrology for Long Range Interferometric Displacement Measurements, " in *Interferometry and Optical Astronomy*, edited by Pierr J. Léna, and Andreas Quirrenbach, Proc. SPIE Vol. 4006, SPIE, Bellingham, WA, 2000, pp. 838-846.

Johnson, L., Gilchrist, B., Estes, R. D., and Lorenzini, E., "Overview of Future NASA Tether Applications," NASA Technical Report 1998-0237034, 1998.

King, L. B., Parker, G. G., Deshmukh, and S., Chong, J., "Spacecraft Formation-Flying using Inter-Vehicle Coulomb Forces," NIAC Phase I Final Report, (2002), www.niac.usra.edu, accessed July 10, 2005.

LaPointe, M. R., "Formation Flight Method," NIAC Phase I Final Report, (2001), www.niac.usra.edu, accessed July 10, 2005.

Lardiere, O., Labeyrie, A., Gillet, S., Riaud, P, "Spaceborne Hypertelescope : A Spacecraft Formation Flying Controlled by Solar Sails," (2002), http://www.arcetri.astro.it/~lardiere/publi/2001-Lardiere-haifa.pdf, accessed April 10, 2006.

Lee, D. et al., "Second Harmonic Generation at 488 nm by Intracavity Doubling of Extended-Cavity Surface-Emitting Lasers," (2004), www.Novalux.com, accessed January 4, 2005.

Leisawitz, D., "A SPECS Update: Engineering and Technology Requirements for a Space-Based Far-IR Imaging Interferometer," *New Frontiers in Stellar Interferometry*, ed. W. A. Traub, Proc. SPIE Vol. 5491, SPIE, Bellingham, WA, 2004, pp. 212-227.

Leitner, J., "Formation Flying – The Future of Remote Sensing from Space," NASA Report, (2004), www.issfd.dlr.de/papers/P0001.pdf, accessed November 11, 2004.

Lorenzini, E. C., Bombardelli, C. and Quadrelli, B. M. 2001, Procs. of 13th AAS/AIAA Space Flight Mechanics Meeting, Paper AAS 03-222, Ponce, Puerto Rico, 9-13 February 2001.

Lovell, R. and O'Malley, T., "Station Keeping of High Power Communication Satellites", NASA TM X-2136, August 1973.

Miller, D.W. and Hall, S R., 1991, Journal of Guidance, Control, and Dynamics, Vol. 14, No. 2, pp. 350- 359.

Miller, D. W., and Sedwick, R. J., "Electromagnetic Formation Flight," NIAC Phase I Final Report, (2003), www.niac.usra.edu, accessed July 10, 2005.

Pain, H. J. , 1983 *The Physics of Vibrations and waves.* Wiley, 3rd edition, p. 156-163.

Palisoc, A.L, "Large Telescope Using a Holographically-Corrected Membrane Mirror," NIAC Phase I Final Report, (2000), www.niac.usra.edu, accessed October 15, 2005.

Phipps, C., Luke, J. R., Helgeson, W. D., "A 25nN Low-Noise Thrust Stand for Microthrusters," International Electric Propulsion Conference IEPC 318 Princeton, NJ October 30-November 4, 310, (2005).

Quinn, D., and Folta, D., "A Tethered Formation Flying Concept for the SPECS Missions," NASA Technical Report 2000-0032752, 2000.

Romanini, D., Kachanov, A.A., Sadeghi, N., and Stoeckel, F., "CW Cavity Ring Down Spectroscopy," *Chem. Phy. Lett.* **264**, 316-322 (1997).

Schielen. E., and Riedl, M., "Diode-Pumped Intracavity Frequency Doubled Semiconductor Disk Laser with Improved Output Beam Properties," Annual Report, (2002), Optoelectronic Dept., Univ. of Ulm, www.opto.e-technik.uni-ulm.de, accessed October 11, 2004.

Schnopper, "Ultarhigh Resolution Fourier Transform X-ray Interferometer," NIAC Fellow Meeting Presentation (2006), http://niac.usra.edu/files/library/meetings/fellows/mar06/1138Schnopper.pdf, accessed March 12, 2006.

Stamper, B. et al., "Flat Membrane Mirrors for Space Telescopes," (2001), caao.as.arizona.edu/publications/ publications/FlatMirror2.pdf.

Woodward, J.F., "Life Imitating Art: Flux Capacitors, Mach Effects, and Our Future in Spacetime," in *Proceedings of Space Tech Applications International Forum (STAIF-2004),* edited by M.S. El-Genk, AIP Conf. Proc. 699, AIP, Melville, N.Y., 2004, pp. 1127-1137.

Woodward, J.F. and Vandeventer, P., "Mach's Principle, Flux Capacitors, and Propulsion," published in this proceeding, 2006.

Yariv, A., *Quantum Electronics*, John Wiley & Sons, New York, New York, 1975, pp. 130-148.

APPENDIX
Publication in STAIF 2006 Proceedings

Space Technology and Applications International Forum, edited by M.S. El-Genk, AIP Conf. Proc. AP813, pp.1213-1223 (2006)*

A Contamination-Free Ultrahigh Precision Formation Flying Method for Micro-, Nano-, and Pico-Satellites with Nanometer Accuracy

Young K. Bae

Bae Institute, 1101 Bryan Ave., Suite C, Tustin, CA 92780, USA, www.baeinstitute.com
714-838-2881, ykbae@baeinstitute.com

Abstract. Formation flying of clusters of micro-, nano- and pico-satellites has been recognized to be more affordable, robust and versatile than building a large monolithic satellite in implementing next generation space missions requiring large apertures or large sample collection areas and sophisticated earth imaging/monitoring. We propose a propellant free, thus contamination free, method that enables ultrahigh precision satellite formation flying with intersatellite distance accuracy of nm (10^{-9} m) at maximum estimated distances in the order of tens of km. The method is based on ultrahigh precision CW intracavity photon thrusters and tethers. The pushing-out force of the intracavity photon thruster and the pulling-in force of the tether tension between satellites form the basic force structure to stabilize crystalline-like structures of satellites and/or spacecrafts with a relative distance accuracy better than nm. The thrust of the photons can be amplified by up to tens of thousand times by bouncing them between two mirrors located separately on pairing satellites. For example, a 10 W photon thruster, suitable for micro-satellite applications, is theoretically capable of providing thrusts up to mN, and its weight and power consumption are estimated to be several kgs and tens of W, respectively. The dual usage of photon thruster as a precision laser source for the interferometric ranging system further simplifies the system architecture and minimizes the weight and power consumption. The present method does not require propellant, thus provides significant propulsion system mass savings, and is free from propellant exhaust contamination, ideal for missions that require large apertures composed of highly sensitive sensors. The system can be readily scaled down for the nano- and pico-satellite applications.

Keywords: formation flying, photon thruster, intracavity, satellite, spacecraft, interferometer, interferometric ranging, propellantless, tether, SPECS, MAXIM, TPF, ST-3, contamination free, micro, nano, pico.
PACS: 07.87.+v, 95.55.-n, 95.55.Fw, 93.85.+q.

INTRODUCTION

In recent years, microsatellites and nanosatellites provide an opportunity to insert sophisticated sensors and processing technologies into orbits of interest at low costs (Leitner, 2004). Building a cluster of small satellites has been recognized to be more affordable, robust and versatile than building a large monolithic satellite. Specifically, the grouped satellite cluster is crucial for enabling orders-of-magnitude improvements in resolution and coverage achievable from advanced remote sensing platforms. Size limitations on launch vehicle fairings leave formation flying as the only option to assimilate coherent large apertures or large sample collection areas in space (Leitner, 2004). For example, for NASA applications, the ultrahigh precision satellite clusters can be used for interferometry and distributed large aperture sensors, especially at optical (TPF, and SPECS) and x-ray wavelengths (MAXIM) (Leisawitz, 2004, Cash, 2002). For non-NASA applications, the proposed system can be used for advanced geophysical monitoring where GPS and standard laser range finders are currently inadequate to measure and

monitor small changes in the movement of earthquake plates, and gravity wave detection. Other commercial and military applications include distributed large aperture optical and infrared sensors for ultrahigh resolution monitoring and imaging at low-cost.

Such a technology critically depends on the formation flying method that enables precision spacecraft formation keeping from coarse requirements (relative position control of any two spacecraft to less than 1 cm, and relative bearing of 1 arcmin over target range of separations from a few meters to tens of kilometers) to fine requirements (nanometer relative position control). For example, one of the most challenging applications for formation flying thus so far is that of the proposed x-ray interferometry for space imaging applications, MAXIM (Cash, 2000). The concept has evolved to include a pathfinder mission, consisting of a single x-ray interferometer and a trailing imaging satellite, and the full MAXIM, consisting of a fleet of 33 x-ray mirror satellites, a trailing collector satellite, and an imaging or detector spacecraft. Summary of the requirement of the baseline accuracy tolerance of several exemplary missions compared with the capability of the present formation flying method is shown in Fig. 1.

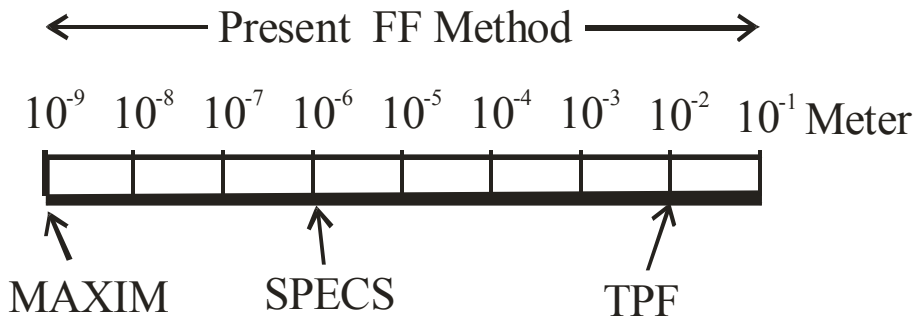

FIGURE 1. Required Base Line Accuracy of Several Exemplary Missions and the Capability of the Present FF Method.

In MAXIM, the relative distance between the hub satellite and collector satellites should be precisely maintained with the tolerance of a few nm (10^{-9}m) at the distance of 200 m, and the precision requirement in maintaining the distance, thus, is 10 parts per trillion, one of the most stringent accuracy requirement seen in any scientific fields. In addition, potential contamination of neighboring spacecraft by propellant exhaust plumes and the possibility of pulsed electromagnetic interference with low power inter-satellite communications remain a real concern for grouped satellite clusters. These requirements essentially rule out the usage of the most of the conventional propellant based propulsion systems, such as gas hydrazine thrusters, pulsed plasma thrusters, hall thrusters, electrostatic ion engines, and field emission electron propulsion systems.

To alleviate these concerns, several propellant-free formation flying methods have been proposed. The propulsive conducting tethers and spin-stabilized tether systems have been proposed in place of on-board propulsion systems to form and maintain satellite formations (Johnson, 1998, Quinn, 2000). While such concepts offer intriguing possibilities for small arrays consisting of only a few spacecraft, implementing a system for dozens of satellites quickly becomes extremely problematic. Several other new concepts have been proposed. They are: 1) the microwave scattering concept (LaPointe, 2001), 2) Coulomb force concept (King, 2002), 3) magnetic dipole interaction concept (Miller, 2003). In the microwave scattering formation flight method (LaPointe, 2001), radiation forces on the order of 10^{-9} N/W may be generated using electromagnetic gradient forces or scattering forces; microwave beam powers of 10-kW can thus produce restoring forces of approximately 10-μN, which are sufficient to correct a number of orbital perturbations. It requires very high power consumption, and focusing of the microwave requires larger antenna arrays, and the scattered microwaves may electronically interfere with other neighboring satellites. The Coulomb control system (King, 2002) is limited to close formation flying in plasma environments characterized by Debye lengths greater than inter-vehicle separation. Even for such formations, however, the Coulomb control forces become negligible for separations greater than 50 m. It is apparent that more traditional thrusters would be necessary for formation keeping over larger distances. Generating usable Coulomb control forces requires charging spacecraft to high voltages, thus great care must be taken in vehicle design to

prevent differential charging and instrument damage due to electrostatic discharge. In the magnetic dipole concept (Miller, 2003), two technical challenges should be overcome: 1) it may not work at the distances greater than tens of meters, thus cannot be used for MAXIM, 2) the system can be extremely bulky and heavy (tons). Therefore, searches continue for the concept that does not require propellant nor extreme high voltages, and is power efficient and light. Very recently, a new form of propellant-free thrust has been investigated and reported to be observed by Woodward (2004) and Woodward and Vandeventer (2006). The usage of such a mechanism for ultrahigh precision formation flying is very interesting, and remains to be investigated.

Even if an efficient propellant-free thrust is developed, for ultrahigh precision formation flying, the issue of thrust pointing, the method of controlling thrust to the desired accuracy, the precision ranging metrology and the overall system architecture should be addressed. The proposed concept in this paper, we believe, satisfies all of these criteria, because:

- The proposed photon thruster system is capable of generating propellant-free continuously for tens of years,
- In combination of a tether system, the proposed photon thruster is capable of controlling and maintaining continuously the intersatellite distance with an accuracy better than nanometer,
- The dual usage of the photon thruster as a laser source for the ultrahigh precision interferometric ranging system simplifies the system architecture and control, and minimizes the system weight and power consumption,
- The thrust vector can be defined with ultrahigh precision due to the nature of the laser cavity.

THE PROPOESED ULTRAHIGH PRECISION FORAMTION FLYING METHOD

The proposed method enables ultrahigh precision satellite formation flying with intersatellite distance accuracy of nm (10^{-9} m) at maximum estimated distances in the order of tens of km. Thus, the present method can be used for most of next generation formation flying missions envisioned so far, including ST-3, TPF, SPECS, and MAXIM. The method is based on innovative ultrahigh precision laser intracavity thrusters able to provide continuously adjustable precision CW thrust between microsatellites and tethers. In slowly spinning systems, as in SPECS, centrifugal force can provide a precise repulsive force, allowing a low-mass tether to provide precise control of distance. There is a problem how quickly that force can be adjusted without risk of inducing undesired resonances, and to solve the problem, the agile control loop can use adjustable laser power rather than mechanical tether length control as the primary control mechanism. In non-spinning systems centrifugal force is not available, and a laser will provide the major repulsive force. In both spinning and non-spinning cases, the fast feedback possible can be used not just to control position, but to reduce the required agility of the tether control, and hence the problems induced by undesired tether resonances.

The schematic diagram of the proposed concept is shown in Fig. 2. Specifically, the proposed formation flying method is based on pulling-in force provided by tether tension and the pushing-apart CW thrust of the intracavity photon thruster. Although the thrust produced by single bounces of photons is typically negligibly small, the intracavity geometry allows photons to bounce between two mirrors as many times as tens of thousands, resulting in several orders of magnitude amplification of the thrust with a given laser power. With this proposed method, we estimate the distance between the satellite pairs in the constellation structure can be adjusted and maintained rapidly to the accuracy of nanometer. The photon thrust and tension of tethers form the backbone linear force structure of the crystalline-like structured formation flying, and can rapidly damp the perturbation from the space environmental sources, such as solar pressure, drag-force, and temperature fluctuation, applied from any direction. Several exemplary structures are illustrated in Fig. 2. For example, the tetrahedral structural can be used for SPECS applications. For MAXIM applications, an elongated polygon bipyramidal structure similar to the 10 satellites constellation can be used, except instead of 8 satellites 32 collector spacecrafts will be used in the plane. The apex will be occupied by the hub and converger crafts. The approximate distance between the collector and hub crafts is about 100 m, and that between the collector and the converger crafts is about 10 km. This is slightly modified structure from the original one (Cash, 2000). These numbers will be used to estimate the necessary operation parameters in the later sections. For one to two dimensional structures, such as in ST-3, multiple photon thrusters and tethers are necessary for a pair of satellites to stabilize the angular disturbance.

More specifically, for SPECS applications, the proposed concept here has two important advantages. First, the usage of tethers will obviate the need for a massive amount of thruster propellant and high-quality imaging interferometry with a 1 km maximum baseline. "High quality imaging" implies the need for dense coverage of the "u-v" plane (i.e., moving the light collecting telescopes to fill the area subtended by the synthetic aperture). To produce images at a reasonable rate, the light collectors will have to be moved around a lot. Although even the most efficient thrusters available can't perform such a task, the tension in a tether can do nearly all the work. Second, to operate with the required sensitivity at far-IR wavelengths, SPECS will have cryogenic optics maintained at 4 K. Therefore, contamination of the optical surfaces is a big concern. The proposed system can be used as an alternative version for the originally proposed for SPECS to overcome these concerns.

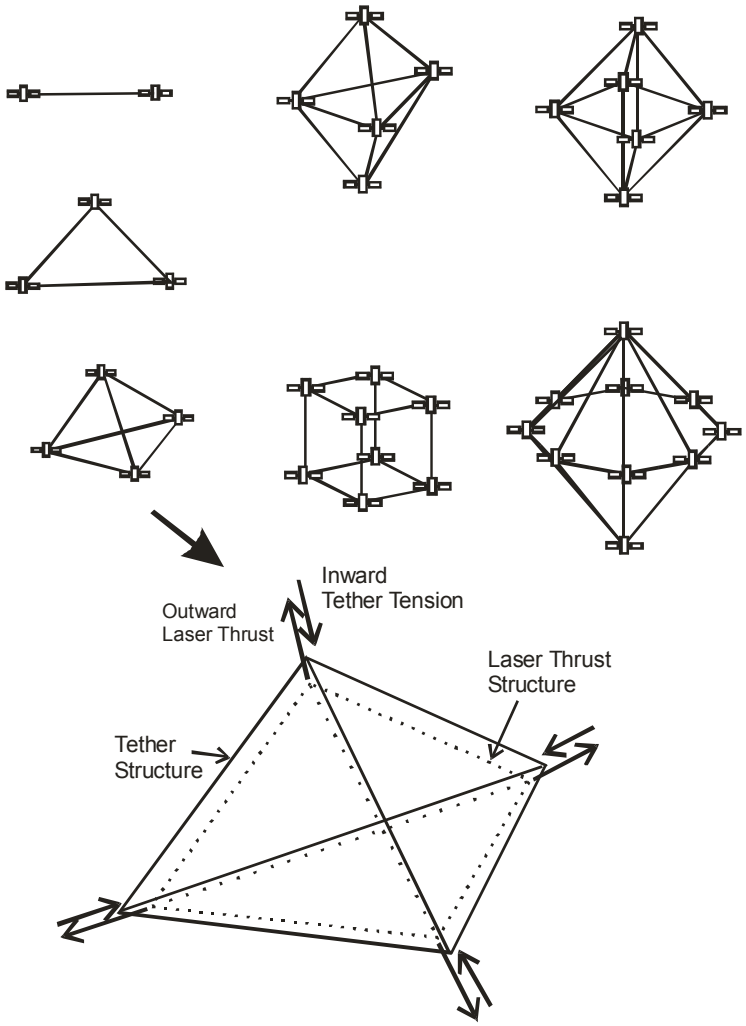

FIGURE 2. Schematic Diagrams of the Exemplary Satellite Mission Configurations with the Proposed Ultrahigh Precision Formation Flying Method.

The more detailed schematic diagram of the system architecture of the proposed system is shown in Fig. 3. The system has three major sub-systems: 1) the photon thruster system, 2) the interferometric ranging system, and 3) the tether system. The proposed ultrahigh precision photon thruster will provide the thrust that will push the satellites apart resulting in Hook's law type extension proportional to the laser thrust. The opposite force is balanced by the tether tension and the length of the tether is proposed to be adjusted by linear translators composed of piezoelectric

translators and stepper motors to the accuracy better than 1 nm. The ultrafine balance of the pulling-in and pushing-apart is maintained by the above two mechanisms and controlled by a computer in real time, forming crystal structure-like satellite cluster. The vibration perturbation or resonance induced by the actuation and motion of the systems and satellites in tether can be rapidly (almost in real time) damped by the photon thruster.

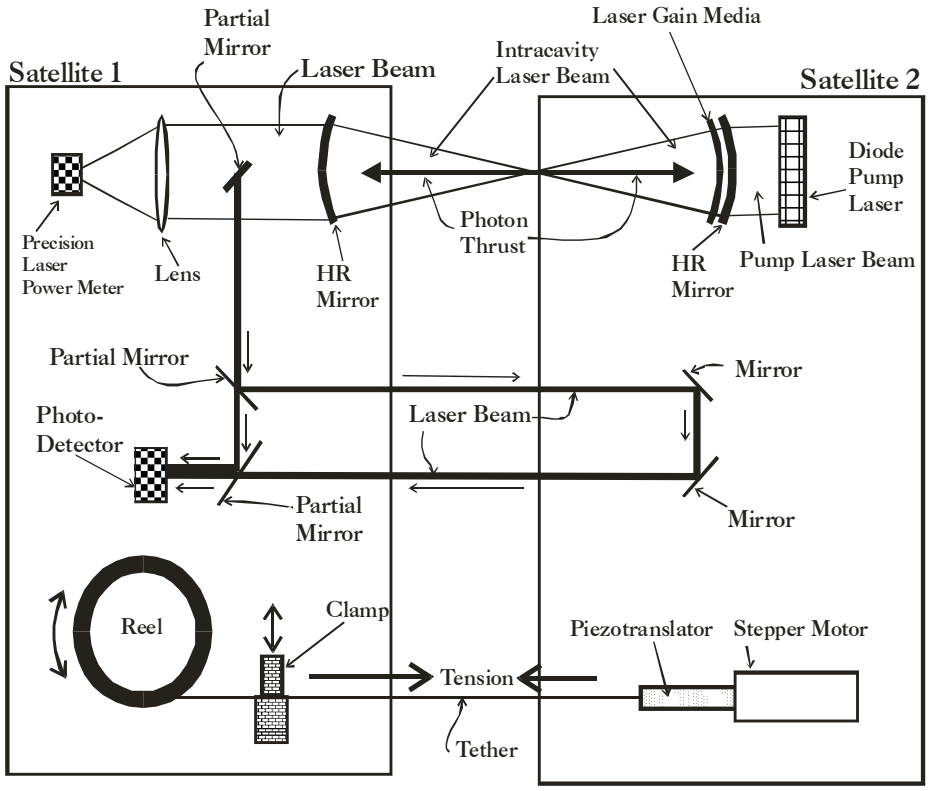

FIGURE 3. Schematic Diagram of the Proposed System Architecture for Pairs of Satellites in Ultrahigh Precision Formation Flying.

For example, diode pumped solid state laser systems, such as a diode pumped YAG laser intracavity laser system, can be used for the proposed formation flying method. In this case, we estimate that the extracavity laser power in the order of 10 W capable of providing photon thrust up to mN is suitable for the weight of each satellite in the order of 100 kg. The power consumption and weight of such a laser system are estimated to be about 30 W and several kg, respectively. The intracavity laser beam is formed between two high reflectance (HR) mirrors located in two separate satellites. The matching tether diameter in this case, for example, is in the order of 0.1 mm with quartz fibers. The power of the laser and the inverse of the cross sectional area of the tether is linearly proportional to the weight of the satellite. For example, the formation of 10 kg and 1 kg satellite constellations, the required laser powers are in the order of 1 W and 0.1 W respectively. The weight of the laser system decreases rapidly as the laser power decreases, thus the technology can be easily adapted to much smaller and lighter satellite platforms.

In the following sections, the details of the subsystems of the proposed formation flying method are given.

The Intracavity Photon Thruster System

In this section the technical details of the intracavity photon thruster system shown in Fig. 3 are presented. The intracavity laser thruster system is proposed to be used to provide ultrahigh precision repulsive force between

satellites against the tether contraction force. If the laser cavity is formed by two mirrors located separately in two satellites, the thrust, F_T, produced by a laser beam on each mirror is given by:

$$F_T = \frac{WRS}{c}, \tag{1}$$

where W the is laser power, c the light velocity, 3 x 10^8 m/s, R the reflectance, and S is the total power enhancement factor that is the ratio of the intracavity laser power to the extracavity laser power. Here, the preferred laser cavity is a confocal resonator that consists of two identical concave spherical mirrors separated by a distance equal to the radius of curvature of the mirrors. The usage of the confocal resonator is much more advantageous than that of a flat mirror resonator. The typical cavity with flat mirrors requires an angular alignment adjustment accuracy of the order of one arc second. However, the confocal resonator has a self-aligning property, thus the alignment requirement requires only about a quarter of a degree, two orders of magnitude less stringent than that with two plane mirrors. Furthermore, the former has much less diffraction loss than the latter (Fowles, 1975).

The total laser power in the intracavity is a function of the reflectance of the HR mirror and other complicated parameters, such as the saturation power of the laser media. Here we consider first the effect of the HR mirror reflectance. Because laser photons are virtually trapped in the intracavity laser formed between two mirrors, the average laser power in the intracavity will be amplified. If there is no saturation of the gain media and no thermal management limitations, the ideal total power enhancement factor, S, of the intracavity is given by:

$$S = \frac{T(1+R)}{(1-R)^2}, \tag{2}$$

where R is the reflectance of the mirror, T is the transmittance through the mirror given by 1 – R –A, and A is the absorption of the mirror coating during reflection. For high quality mirrors, A ~ 10^{-6}, thus, for the R < 0.99999, T ~ 1 – R, and the Equation (1) becomes:

$$F_T \approx \frac{2W}{(1-R)c}. \tag{3}$$

The parameters that determine the maximum attainable intracavity laser power are:

- The power saturation of the gain media
- The thermal management capacity of the gain media
- The HR mirror manufacturing consistency

For estimating the theoretical limit maximum intracavity laser power and the corresponding thrust, the other parameters are neglected, and results of the maximum theoretical thrusts as a function of the reflectance of the mirrors at the extracavity laser power of 10 W are summarized in Table 1.

TABLE 1. The Maximum Theoretical Thrusts of the Photon Thruster as a Function of the Mirror Reflectance at the Extracavity Laser Power of 10 W.

Maximum Operation Laser Power (extracavity)	HR Mirror Reflectance	Maximum Theoretical Thrust
10 W	0.90 - 0.99 (commonly used in laser cavities)	0.67 - 6.7 μN
10 W	0.999 (used in laser cavities)	67 μN
10 W	0.9999 (research grade)	0.67 mN
10 W	0.99995 (typically used super mirror)	1.34 mN

The optimum design of the proposed intracavity photon thruster is different from that of the typical laser cavities. The cavity design of the typical lasers is tailored to maximize the laser output power in the extracavity. Depending

on the characteristics of the gain media, the reflectance of the output mirror (output coupler) is chosen 0.9 – 0.99 for the conventional laser cavities. In some cases the HR mirror with the reflectance of 0.999 has been used (Lee, 2005). To minimize the absorption loss in the gain media, the proposed photon thruster should be designed to maximize the intracavity power, thus the gain media should be very thin to minimize the absorption loss in the gain media, similar to the one used in the state of the art solid state disk lasers used for intracavity second harmonic generation, except without the need of the frequency doubling crystal (Schielen, 2004). In this case, the thermal management of the gain media becomes an important issue.
In this analysis, we have only considered the reflectivity and absorption loss of the mirrors, however, several other factors including thermal limitation and optical absorption and saturation of the laser gain media have to be considered. In reality, because of the limitation in the laser gain medium and other thermal effect, the total thrust presented in Table 1 should be considered as upper bounds. The current off-the-shelf technological limit of the system reported to date is obtained with super mirrors used for the cavity ring down spectroscopy (Romanini, 1997) (currently available in the advanced research grade only) with the reflectance of 0.99995.

The maximum thrust of the proposed photon thruster as a function of the mirror reflectance, R, is shown in Fig. 4. Note that the x-axis represents 1/(1-R), which is approximately proportional to the number of reflections between two mirrors of the photon thruster. The photon thrust shown here is calculated for a 10 W laser system, and the higher laser power will reduce the required value for 1/(1-R) proportionally. The approximate perturbation forces applied to the satellite pair of several exemplary formation flying structures due to solar radiation pressure or gravitational perturbation are shown in Fig. 4.

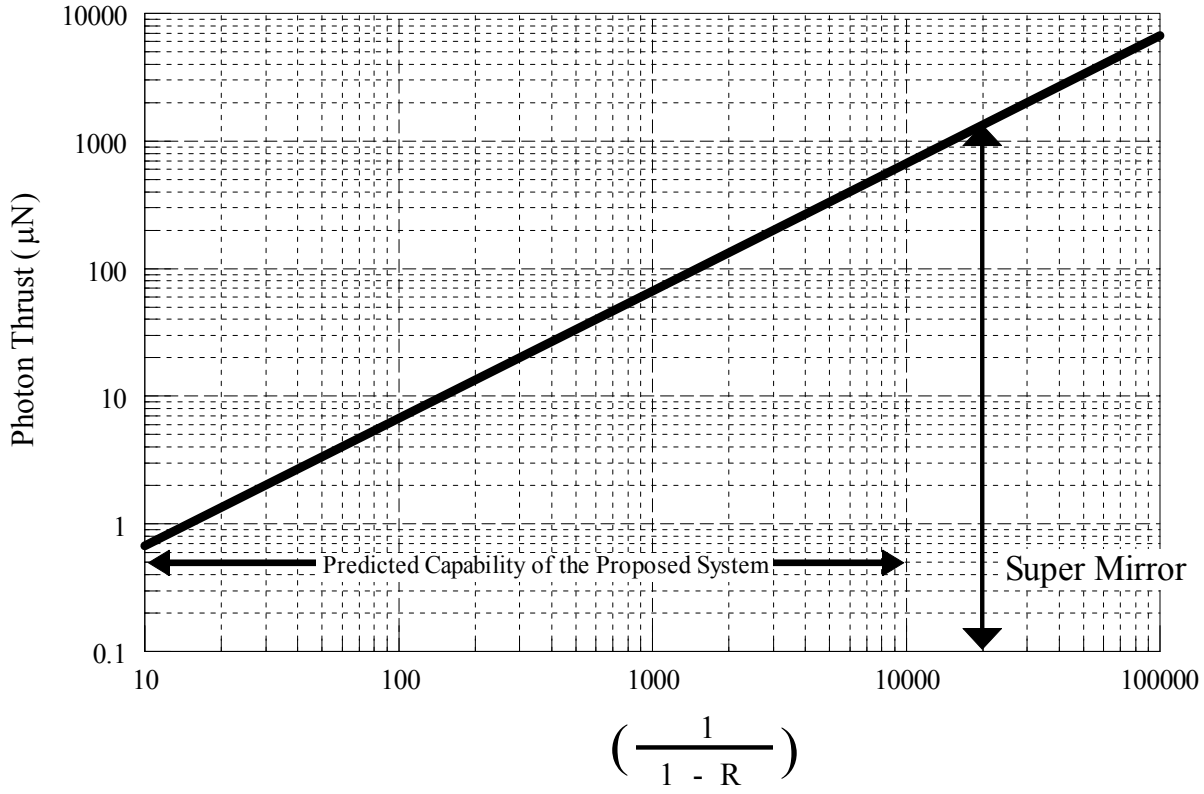

FIGURE 4. The Maximum Thrust of the Proposed Photon Thruster of 10 W as a Function of the Mirror Reflectance, R.

Based on the currently available laser technology, by making the gain media thin enough, the photon thruster with 0.999 -0.9999 is predicted to be readily possible with the laser design optimized for maximizing the intracavity

power in the near future. With this, 10 W photon thrusters are predicted to be able to deliver up to 670 μN, which is large enough to compensate various perturbations in the space environment for most of missions envisioned as shown in Fig. 4. We note that the achievement of such high photon thrust will require highly sophisticated gain medium and pumping design and engineering, which is predicted to be within reach in the near future.

Dual Usage of the Photon Thruster for the Interferometric Ranging System

The next generation formation flying will require a highly sophisticated ranging system for monitoring the intersatellite distance. One of the best candidates for the ranging system for the proposed ultrahigh precision formation flying method is the laser interferometric ranging system (Jeganathan, 2000, Bender, 2003). We propose here the dual usage of the photon thruster as a laser source of the interferometric ranging system. Fig. 3 illustrates the schematic diagram of the proposed subsystem in which a portion of the extracavity laser beam is reflected by a partially reflecting mirror (or a fully reflecting mirror) to be used for interferometric ranging. The schematic diagram represents one of many possible designs, and the selection of the most suitable system may depend on the specific mission requirement. The interference of the primary laser beam in the primary satellite and the laser beam reflected by the mirrors in the secondary satellite is used for assessing the relative distance change between the satellites. This dual usage will significantly simplify the system design and reduce the system weight and power consumption.

Lifetime of the Proposed Intracavity Laser System

When the interferometer in the satellite cluster operates, the intracavity laser should operate continuously to dynamically adjust the relative distances and bearings between the satellites. The lifetime of the formation system is thus limited by the lifetime of the laser system. Currently, the lifetime of the diode pumped solid state lasers at full operation power is limited by that of pump diodes to about 10,000 hours (1 year) continuous operation. At the reduced power operation the lifetime of the pump diodes is expected to be longer. The overall lifetime of the system can be further extended by simply replacing the pump diodes with new ones. The alignment of the pump diodes does not have to be precise; a design with carousels of pump diodes can be easily made. With a ten unit carousel, for example, the lifetime of the system is extended to tens of years. With the rapidly developing diode laser technology, the lifetime is expected to increase significantly over the next decade.

The Tether System

The proposed intracavity laser system will be combined with a tether system that will provide pulling-in force between a satellite pair through tension. For the gross length adjustments of the tether, in one of the pair satellite is proposed to have a reel mechanism and inchworm actuator that can be clamped to or released from the tether to allow low-noise fine adjustments (Fig. 3). The tether will be extended with the use of laser thrust that will be counterbalanced by the tether tension. The other satellite in the pair is proposed to have a piezoelectric translator with sub nm accuracy. Currently, off-the-shelf piezoelectric translator can deliver the accuracy resolution of 0.02 nm. Because the accuracy in the distance maintenance relies on that of the piezoelectric translator, the proposed system will be able to deliver the sub nm accuracy. The variation in length Δl_F with the tension F, which is counterbalanced by laser thrust, is given by:

$$\Delta l_F = \frac{1}{Y}\frac{F}{A}l, \tag{4}$$

where Y is the Young's modulus, A is the cross sectional area of the tether, and l is the length of the tether.

Many exemplary mission systems can use the proposed formation flying method. As an example, we will consider a system that consists of satellites with an intersatellite distance of 200 m and the distance accuracy in the order of 1 nm. The system has intracavity photon thrusters with 10 W capacity with the mirror reflectance, R=0.999, capable

of producing the intersatellite thrusts up to 67 μN. The tethers are made of quartz, and have a diameter of 100 μm. We assume the maximum perturbation force on each satellite is 10 μN, thus the maximum perturbation force on a satellite pair is 20 μN as shown in Fig. 4. In this system, to maintain the intersatellite distance in the accuracy of 1 nm at a distance of 200 m with a quartz tether with a diameter of 100 μm ($A = 7.85 \times 10^{-9}$ m^2) and $Y = 5.4 \times 10^{10}$ Pa, the system should be able to provide the thrust accuracy in the order of 2 nN (2×10^{-9} N). One way to maintain such an accuracy is that the tether is stretched by the constant photon thrust of 30 μN in average (in length of 15 μm), and the perturbative force is counter balanced by changing the photon thrust or the tether tension by moving the piezoelectric translators. In this case, because the piezoelectric translators have the resolution much better than 1 nm, the limiting step is the photon thruster power accuracy, and to obtain 1-nm accuracy, the photon thrusters should have the noise to main power ratio in the order of 10^{-5}. In the currently available CW laser systems, such noise to main power ratio can be achieved. Theoretically, either the photon thruster power or the piezoelectric translator can be continuously controlled in real time by the feedback distance signal from the laser interferometers that measure and monitor the intersatellite distance continuously. Therefore the proposed intracavity thruster system, in principle, can provide the distance adjustment better than nanometer accuracy.

In another example, a system considered has an intersatellite distance of 1 km and the distance accuracy in the order of 1 μm. The system has intracavity photon thrusters with 10 W capacity with the mirror reflectance, R= 0.9995, capable of producing the intersatellite thrust up to 134 μN. The similar thrust can be achieved by the system with R=0.999 and 20 W photon thruster power. We assume the maximum perturbation force on each satellite is 50 μN, thus the maximum perturbation force on a satellite pair is 100 μN. See Fig. 4. In this system, to maintain the intersatellite distance in the accuracy of 1 μm at a distance of 1,000 m with a quartz tether with a diameter of 100 μm ($A = 7.85 \times 10^{-9}$ m^2) and $Y = 5.4 \times 10^{10}$ Pa, the system should be able to provide the thrust accuracy in the order of 4.2 μN. One way to maintain such an accuracy is that the tether is stretched by the constant photon thrust of 100 μN (23.8 μm in length) in average, and the perturbative force is counter balanced by changing the photon thrust or the tether tension by moving the piezoelectric translators. The accuracy requirement is only 0.042, thus readily achievable with the present proposed system. The ultimate intersatellite distance accuracy achievable with the current system by assuming the laser power noise in the order of 10^{-5}, is 0.24 nm.

Thermal Contraction/Expansion of the Tether System

One of important problems that the tether based system will encounter is thermal expansion/contraction of the tethers due to exposure or non-exposure of sunlight. In fact, this thermal expansion/contraction is the key factor that limits the usage of any formation methods relying on solid monolithic structured beds, in which the engineering of the real-time response system to the thermal effect is daunting. However, the proposed system with tethers and photon thrusters has a built-in capability of responding to such thermal perturbation. In the proposed tether system, the length change Δl_t resulted from the temperature change Δt is given by:

$$\Delta l_t = \beta l \Delta t \,. \tag{5}$$

For example, at l = 200 m an environmental temperature change, Δt =10 C, will result in the tether length change as much as 1.1 mm. This temperature fluctuation will be readily compensated by a piezoelectric linear translator coupled to the tether in the similar fashion to the force perturbation. The interferometer monitors the change and provides the feedback signal that controls the piezoelectric translator for compensation. If the temperature change results in the tether length changes greater than the dynamic range of the piezoelectric translator, a reel and/or stepper motor system will kick in to provide much larger dynamic range.

Maximum Range of Operation, Deployment and u-v Plane Activity Related Issues

The maximum range of the operation of the proposed system depends on the diameter of mirrors. The theoretical limit of the intracavity length, L, for a confocal cavity resonator is given by (Yariv, 1975):

$$L = \frac{r_1 r_2}{\lambda}, \tag{6}$$

where r_1 and r_2 are the radii of the laser beam projected on the mirrors, and λ is the wavelength of the laser. For example, for MAXIM applications with L=200 m, the required minimum diameter of mirror is 3 cm. The required minimum diameter of mirrors for the photon thrusters as a function of the operation distance is given in Table 2. The deployment process of the proposed system can be achieved by firing the photon thruster at programmed thrust until the satellites establish a desired initial intersatellite distance, while the pointing/alignment of the laser is actively controlled by the mirror controlling system and the tether is gradually released. In the most of the envisioned missions, the need for dense coverage of the u-v plane requires continuously variable operation distance. In addition, in some missions, repeatable satellite segmentation/desegmentation may be necessary.

TABLE 2. The Distance of Operation and the Required Diameter of Mirrors for the Photon Thruster Operation.

Distance of Operation	Required Minimum Diameter of Mirrors
200 m*	3 cm
1 km	6.4 cm
10 km**	20.2 cm

*Maximum distance between the collector and hub crafts in MAXIM.
** The distance between the hub (or collector) and converger crafts in MAXIM.

So far, we have considered the design and performance of the proposed system at the maximum intersatellite operation distance. Because the curvature and radius of the mirrors of the proposed formation flying method are designed for the maximum baseline distance, during deployment process and u-v plan activities at shorter distances, the laser beam in the cavity will be defocused. In this case, the characteristics of the laser cavity will be in between that of the confocal cavity and that of the flat mirror cavity. The fractional power loss per transit of the laser beam in the intracavity is a function of the Fresnel number, N given by (Fowles, 1975):

$$N = \frac{r_1 r_2}{\lambda L}, \tag{7}$$

where L is the length of the laser cavity, r_1 and r_2 are the radii of the laser beam projected on the mirrors, and λ is the wavelength of the laser. In the proposed system, r_1, r_2 and λ are constant, thus N is inversely proportional to L. The fractional power loss per transit is a function of N, and for the confocal cavity, it is a rapidly exponentially decreasing function of N, while for the flat mirror cavity, it is a slowly exponentially decreasing function of N (Fowles, 1975). At shorter operation distances, as N increases, the curve of the fractional power loss per transit shift from that of the confocal cavity to that of the flat cavity. At very short operation distances, particularly during the initial deployment, the laser cavity is close to that formed by flat mirrors. These effects of increased N and the shift of curves on the fractional power loss per transit in the laser cavity are expected to compensate each other; however, the degree of compensation is not known currently. If the effect of the increased N on the fractional power loss per transit under-compensates that of the curve shift, the increase of the mirror diameter is necessary. The details of the optical analysis of these issues are currently underway.

CONCLUSION

We have presented general engineering requirements, design concepts, possible implementation approaches, and technology requirements for a novel propellant free, thus contamination free, method that enables ultrahigh precision satellite formation flying with intersatellite distance accuracy of nm (10^{-9} m) at maximum estimated distances in the order of tens of km. In particular, the proposed method takes advantage of the dual usage of the photon thruster as a laser source for the laser interferometric ranging system for monitoring intersatellite distances in greatly reducing the complexity of the system design, weight, and power consumption. The proposed formation flying method is expected to expedite the realization of many new space missions and sophisticated earth imaging/monitoring, and to open a new class of space missions based on groups of micro-, nano, and pico satellites.

We have also shown that the proposed formation flying method is within the currently available technology, and that with the laser technology specifically optimized for the proposed method will improve its efficiency by orders of magnitude in the near future. The detailed mission-specific technical analyses and supporting engineering studies on the outstanding technical issues are currently underway.

NOMENCLATURE

A = cross sectional area of tethers (m^2)
β = thermal expansion coefficient (K^{-1})
c = vacuum speed of light (m/s)
l, l_F, l_t = tether length (m)
F = force (N)
F_T = thrust (N)
L = length of the laser cavity (m)
λ = wavelength of the laser photon (m)
r_1, r_2 = radii of the laser beam projected on the mirrors (m)
R = mirror reflectance
S = total laser power enhancement factor in the laser cavity
t = temperature (K)
T = transmittance through the mirror
W = laser power (W)
Y = Young's modulus (N/m^2)

ACKNOWLEDGMENTS

The author thanks Drs. J. Leitner, D. Leisawitz, W. C. Larson, and F. Mead for their highly encouraging discussions and suggestions. The present work is supported by NASA Institute for Advanced Concepts (NIAC) under Research Subaward No. 07605-003-041 of NASA Contract NAS5-03110 and Bae Institute internal research funding. In particular, the encouragement of Dr. R. Cassanova, Director of NIAC, is greatly appreciated.

REFERENCES

Bender, P.L., Hall, J.L., Ye, J., and Klipstein, W.M., "Satellite-Satellite Laser Links for Future Gravity Missions," *Space Sci. Rev.* **108**, 377-384 (2003).

Cash, W., "X-ray Interferometry-Ultimate Imaging," NIAC Phase II Final Report, (2002), www.niac.usra.edu, accessed July 10, 2005.

Fowles, G. R., *Introduction to Modern Optics*, Holt, Rinvehart and Winston, Inc., New York, New York., 1975, pp. 278-281.

Jeganathan, M., and Dubovitsky, S., "Demonstration of nm-level Active Metrology for Long Range Interferometric Displacement Measurements, " in *Interferometry and Optical Astronomy*, edited by Pierr J. Léna, and Andreas Quirrenbach, Proc. SPIE Vol. 4006, SPIE, Bellingham, WA, 2000, pp. 838-846.

Johnson, L., Gilchrist, B., Estes, R. D., and Lorenzini, E., "Overview of Future NASA Tether Applications," NASA Technical Report 1998-0237034, 1998.

King, L. B., Parker, G. G., Deshmukh, and S., Chong, J., "Spacecraft Formation-Flying using Inter-Vehicle Coulomb Forces," NIAC Phase I Final Report, (2002), www.niac.usra.edu, accessed July 10, 2005.

Lee, D. et al., "Second Harmonic Generation at 488 nm by Intracavity Doubling of Extended-Cavity Surface-Emitting Lasers," (2004), www.Novalux.com, accessed January 4, 2005.

LaPointe, M. R., "Formation Flight Method," NIAC Phase I Final Report, (2001), www.niac.usra.edu, accessed July 10, 2005.

Leisawitz, D., "A SPECS Update: Engineering and Technology Requirements for a Space-Based Far-IR Imaging Interferometer," *New Frontiers in Stellar Interferometry*, ed. W. A. Traub, Proc. SPIE Vol. 5491, SPIE, Bellingham, WA, 2004, pp. 212-227.

Leitner, J., "Formation Flying – The Future of Remote Sensing from Space," NASA Report, (2004), www.issfd.dlr.de/papers/P0001.pdf, accessed November 11, 2004.

Miller, D. W., and Sedwick, R. J., "Electromagnetic Formation Flight," NIAC Phase I Final Report, (2003), www.niac.usra.edu, accessed July 10, 2005.

Quinn, D., and Folta, D., "A Tethered Formation Flying Concept for the SPECS Missions," NASA Technical Report 2000-0032752, 2000.

Romanini, D., Kachanov, A.A., Sadeghi, N., and Stoeckel, F., "CW Cavity Ring Down Spectroscopy," *Chem. Phy. Lett.* **264**, 316-322 (1997).

Schielen. E., and Riedl, M., "Diode-Pumped Intracavity Frequency Doubled Semiconductor Disk Laser with Improved Output Beam Properties," Annual Report, (2002), Optoelectronic Dept., Univ. of Ulm, www.opto.e-technik.uni-ulm.de, accessed October 11, 2004.

Woodward, J.F., "Life Imitating Art: Flux Capacitors, Mach Effects, and Our Future in Spacetime," in *Proceedings of Space Tech Applications International Forum (STAIF-2004),* edited by M.S. El-Genk, AIP Conf. Proc. 699, AIP, Melville, N.Y., 2004, pp. 1127-1137.

Woodward, J.F. and Vandeventer, P., "Mach's Principle, Flux Capacitors, and Propulsion," published in this proceeding, 2006.

Yariv, A., *Quantum Electronics*, John Wiley & Sons, New York, New York, 1975, pp. 130-148.